ISSN 0035—922X

JOURNAL OF THE ROYAL SOCIETY OF WESTERN AUSTRALIA

VOLUME 64

PART 2

AUGUST, 1981

PRICE THREE DOLLARS

REGISTERED FOR POSTING AS A PERIODICAL—CATEGORY B

THE ROYAL SOCIETY OF WESTERN AUSTRALIA

PATRON

Her Majesty the Queen

VICE-PATRON

His Excellency Rear Admiral Sir Richard Trowbridge, K.C.V.O., K.St.J., Governor of Western Australia

COUNCIL 1980–1981

President ..... J. R. de Laeter, B.Ed. (Hons.), B.Sc. (Hons.), Ph.D., F.Inst.P., F.A.I.P.

Vice-Presidents ..... J. F. Loneragan, B.Sc., Ph.D., F.T.S.
A. E. Cockbain, B.Sc., Ph.D.

Past President ..... M. J. Mulcahy, B.Sc. (For.), Ph.D.

Joint Hon. Secretaries ..... P. Bridgewater, B.Sc., Ph.D.
A. Petch, B.Sc. (Agric.) (Hons.)

Hon. Treasurer ..... S. J. Curry, M.A.

Hon. Librarian ..... H. E. Balme, M.A., Grad. Dip. Lib. Stud.

Hon. Editor ..... A. E. Cockbain, B.Sc., Ph.D.

D. T. Bell, B.A., Ph.D.

S. J. J. F. Davies, M.A., Ph.D.

S. D. Hopper, B.Sc. (Hons.), Ph.D.

C. F. H. Jenkins, M.B.E., M.A., M.A.I.A.S.

L. E. Koch, M.Sc., Ph.D.

L. J. Peet, B.Sc., Dip. Val., Dip. R.E.M., F.G.S., A.R.E.I.

P. E. Playford, B.Sc., Ph.D.

P. R. Wycherley, O.B.E., B.Sc., Ph.D., F.L.S.

Journal of the Royal Society of Western Australia, Vol. 64, Part 2, 1981, pp. 33-51.

The geomorphology and surface processes of the Australind-Leschenault Inlet coastal area

by V. Semeniuk and T. D. Meagher

21 Glenmere Road, Warwick, W.A. 6024.
8 Talgarth Way, City Beach, W.A. 6015.

Manuscript received 19 February 1980; accepted 18 March 1980

Abstract

The Australind-Leschenault Inlet area, near Bunbury Western Australia, is in the southern part of the Swan Coastal Plain. The development of the geomorphology is related to the physical features of climate (rainfall, the evapo-transpiration regime and wind) and oceanography. Wind is an important element in that it mobilises sand and also generates local waves. Tidal influence is minimal and the main oceanographic features include a wave-dominated coast subject to swell and wind waves, and a protected lagoon subject to locally generated wind waves.

Four major geomorphic units are recognised: (1) a hinterland, composed of Bassendean, Spearwood and Blythewood units; (2) Leschenault Inlet, a narrow lagoon; (3) Leschenault Peninsula, which is a narrow barrier of dunes referable to the Quindalup system and (4) a nearshore submarine shelf. Three of these units are further divided into geomorphic sub-units. The Leschenault Inlet system contains samphire and sedge (tidal) flats, sand shoals and platforms and an interior basin. The Leschenault Peninsula contains a beach/beach ridge system on the western side, mobile and fixed dunes over most of its surface and predominantly vegetated dunes and woodland plains on its eastern side. On the peninsula there is contemporary development of soils and subsurface cementation. The submarine shelf is underlain mainly by Tamala Limestone and ridges of beachrock; locally there are outcrops of basalt and relic muddy estuarine deposits. Beachrock is forming in the subsurface along the shoreface of the peninsula and is exposed by periodic coastal retreat.

Major processes important to the development of Holocene geomorphology are sedimentation and erosion. Sedimentation sites include (1) Leschenault Inlet, (2) the zone of dune encroachment along the eastern side of the peninsula and (3) local pockets of beach-ridges. Mobile dunes ultimately spill into the inlet and thus there is a progressive migration of the barrier across the inlet. Wind and wave erosion however are prevalent and dominant processes in developing the coastal morphology (steep cliffed dune line, eroding hollows) and the submarine shelf morphology. Removal of sediment in the shore zone results in a nearshore beachrock ridge system left in the wake of coastal retreat and an offshore pavement of Tamala Limestone. The bulk of the coastal sediment is moving in a net northerly direction out of the study area.

Introduction

The region of Australind-Waterloo Head-Leschenault Inlet-Koombana Bay (near Bunbury) on the southern portion of the Swan Coastal Plain (Fig. 1) contains a number of landform units, Pleistocene to Holocene in age (McArthur and Bettenay 1960). As a result of research in this area new information was obtained that adds to the detail on the geomorphic evolution of the coastline. The data also gives insight into some processes of coastal development on the broader context of the Swan Coastal Plain.

The data and interpretations will be presented in a series of papers on various inter-related aspects of natural history of the area. This paper presents the geomorphic framework essential to the appreciation of other papers on stratigraphy and geologic history (Semeniuk in prep.) and habitats and biology (Semeniuk and Blackwell in prep.). As such this paper describes the main geomorphic units and the key processes important to the development of the area.

Methods

A broad range of techniques was used to assemble the data presented here. These included:

1. A review of the aerial photographic record taken over the area in 1940, 1966, 1971, 1974 and 1978. The photographs are available from the Western Australian Department of Lands and Surveys.
2. The identification and surface mapping of the major geomorphic and stratigraphic units.
3. An examination of the near-surface stratigraphy in 55 small backhoe excavations, in 8 large costeans made by bulldozer and drag line, and along wind and wave-eroded cliff faces particularly after some severe storms.
4. An examination of the seafloor topography and stratigraphy by diving. Samples of the seafloor bedrock were collected by blasting.

(1)—11558

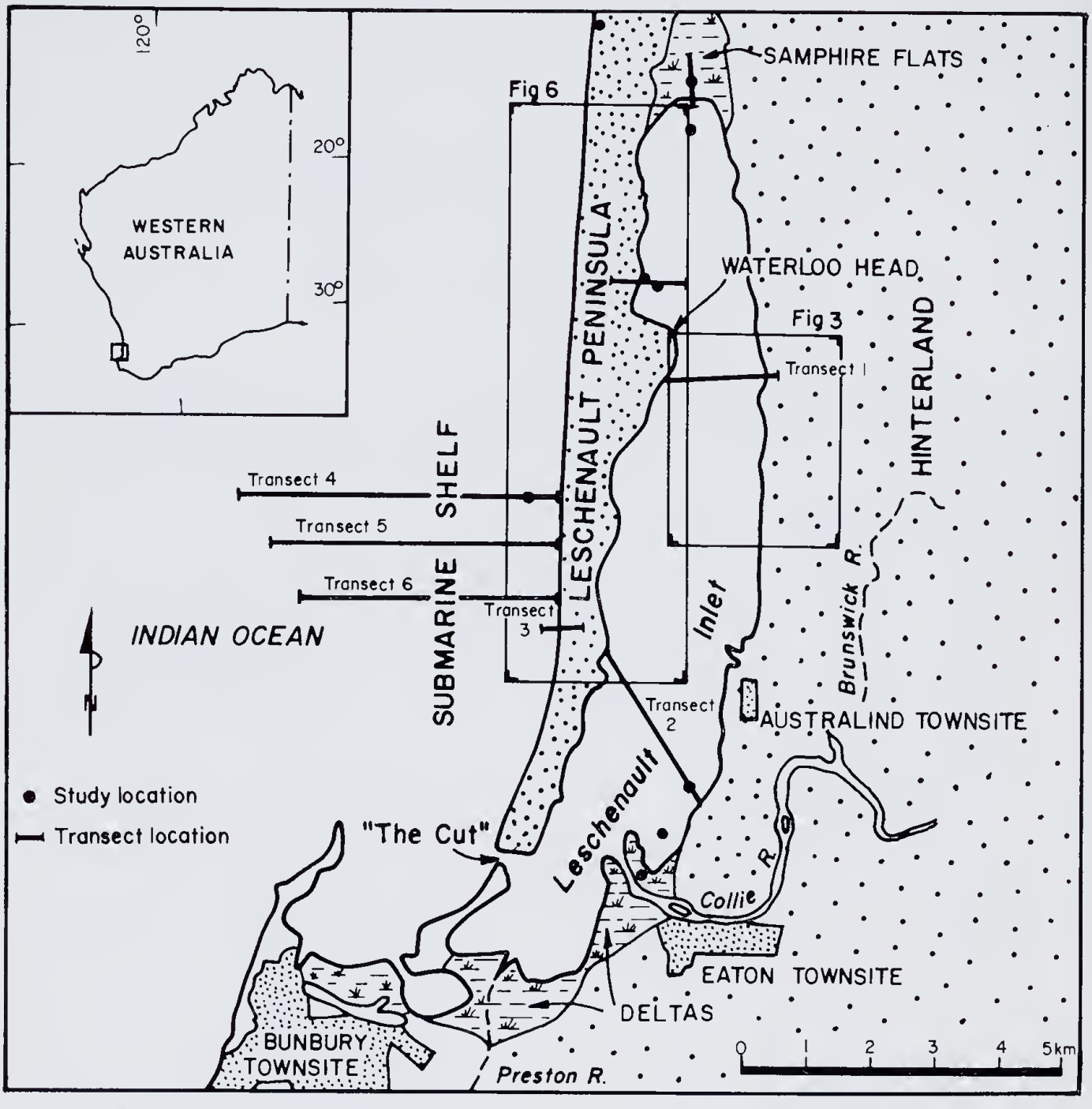

Figure 1.—Map of study area showing main geomorphic units and geographic features mentioned in text. Locations of more detailed maps, transects and study sites also are shown.

5. Coring to depths of 8-30 m with both diamond drill and percussion-coring devices to obtain some 70 cores; core data are presented in Semeniuk (in prep.).

6. Documentation by observation and photography of the modern surface and near-surface processes; this has elucidated the mechanisms by which the stratigraphy, hydrology, geochemistry and biology have developed. Some of these data provide analogues of material found in core.

From these sample sites, some 2 000 sediment samples were collected and examined under binocular microscope for structure, fabric, texture and gross (mineral) composition. Selected samples were disaggregated under the microscope and tested for carbonate with hydrochloric acid. Standard laboratory analyses were made on some samples; these included: grain-size analysis by seiving and thin section (48 samples), X-ray diffractometry (16 samples), chemical analyses for calcium carbonate and ferrous iron content (62 samples). An additional 200 sediment samples from selected intervals at depth have been analysed for a range of constituents by the Government Chemical Laboratories. These results were incorporated in our study of sedimentary profiles.

Regional setting

The processes influencing the formation of landforms today are related to the physical phenomena of climate (rainfall, evaporation and wind) and oceanography. These also influence the distribution of sediment types and the formation of stratigraphic units. The physical characteristics of the environment essential to the geomorphic processes are outlined below.

Climate

The climate of the area is typically Mediterranean with hot dry summers and mild wet winters. Annual precipitation is 881 mm (average) falling mainly in April to November. Temperatures reach a mean maximum of 27.9°C in January. The corresponding mean maximum for winter occurs in August at 16.5°C. The mean minimum temperature in winter is 8.3°C. Climatic data are presented in Table 1 (Bureau of Meteorology 1975).

Wind is important in this area for its role in movement of sand and in the generation of waves along beach faces. Measurements of wind collected at Bunbury (Steedman pers. comm. 1979) summarise the wind regime for the study area (Table 2 and Figure 2B). Analysis shows clearly the division between the summer and winter wind patterns prevailing over the region. Normal wind patterns are related to the position of the eastward-travelling high and low pressure systems which control the weather (Gentilli 1972).

The winter period is characterised by storms with intervening relatively calm weather. The storms typically have mean wind speeds up to 20 m/s for 6-24 hour durations, and mainly prevail from the north-west, west and south-west sectors. Two to four of these storms may be expected each winter, with minor storms occurring approximately every 2 weeks.

As summer approaches the high pressure systems move north and the regional wind conditions moderate. Sea breeze/land breeze systems then control the winds in the coastal area. This results as the differences between the land and sea temperatures dominate the winds, particularly in the summer afternoon periods when the sea breeze blows from the west to south-west with speeds up to 15 m/s.

During the summer there is the possibility of tropical cyclones travelling through the area. Although they are weakening, these storms are still capable of producing extreme wind and waves. Late summer to autumn is the calmest period of the year with light winds.

The important elements of the wind pattern in moving sand are that in summer wind blows onshore during the afternoon with far more strength and duration than does the opposing wind from the land. Figure 2 shows that sand-shifting speeds (i.e. > 4.5 m/s) near ground level occur predominantly from south-west to north-west quarters associated with sea

Table 1

Climatic data for Bunbury (from Bureau of Meteorology 1975)

Unit	Jan	Feb	Mar	Apr	May	Jun	Jul	Aug	Sep	Oct	Nov	Dec	Year
Mean rainfall (mm)	10	12	23	46	129	186	174	126	81	55	25	14	881
Mean no. raindays	3	3	4	8	14	18	20	17	14	11	6	4	122
Daily mean maximum temperature (°C)	27·4	27·9	25·6	21·7	19·6	17·5	16·7	16·5	17·6	20·1	22·3	25·9	21·6
Daily mean minimum temperature (°C)	16·5	16·6	14·9	12·9	10·7	9·8	9·1	8·3	9·5	10·9	12·7	15·0	12·2
9 a.m. mean relative humidity (%)	63	62	67	77	75	81	78	76	73	67	65	63	71
3 p.m. mean relative humidity (%)	59	54	57	64	62	69	69	67	64	62	61	59	62

Table 2

Annual wind velocity data, Bunbury Power Station, January to December 1977. *The body of the table shows the relative frequency as a percentage.*

Direction(²)	Wind speed (m/s)(¹)								
	0–2	2–4	4–6	6–8	8–10	10–12	12–14	>14	Totals
North	0·6	0·9	2·2	1·1	0·4	0·3	0·2	0·3	5·8
North-east	0·9	1·3	1·6	0·3	0·1	*	*	*	4·4
East	3·0	2·7	3·4	0·6	0·1	*	*	*	9·9
South-east	5·4	4·5	6·9	2·0	0·3	0·1		*	19·2
South	6·1	5·4	7·4	1·9	0·4	0·1			21·3
South-west	2·5	2·5	4·2	1·1	0·3	0·1	*	*	10·7
West	0·9	1·3	6·8	3·7	1·6	1·0	0·4	0·3	16·0
North-west	0·6	1·1	3·5	2·3	1·5	0·9	0·5	0·4	10·8
Totals	20·0	19·8	36·0	13·0	4·7	2·6	1·1	1·0	

Percentage calm = 1·9 No. of readings = 8 752

Note:

* Denotes occurrence is <0·05%.

(¹) Speed,s, in e.g. group 2–4 implies $2{\cdot}0 < s \leq 4{\cdot}0$ etc.

(²) Direction groups 22·5 ° either side of specified direction.

(2)—11558

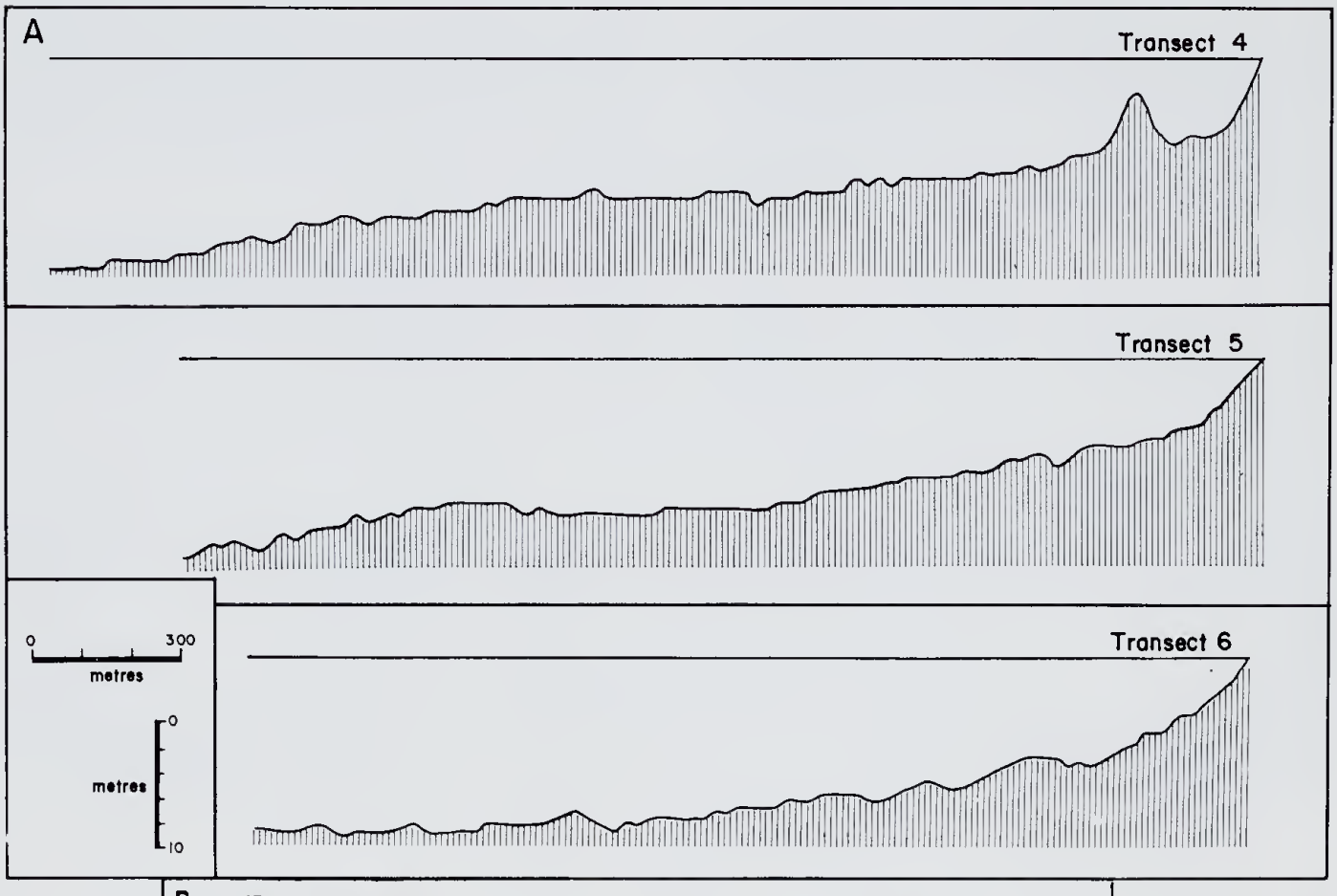

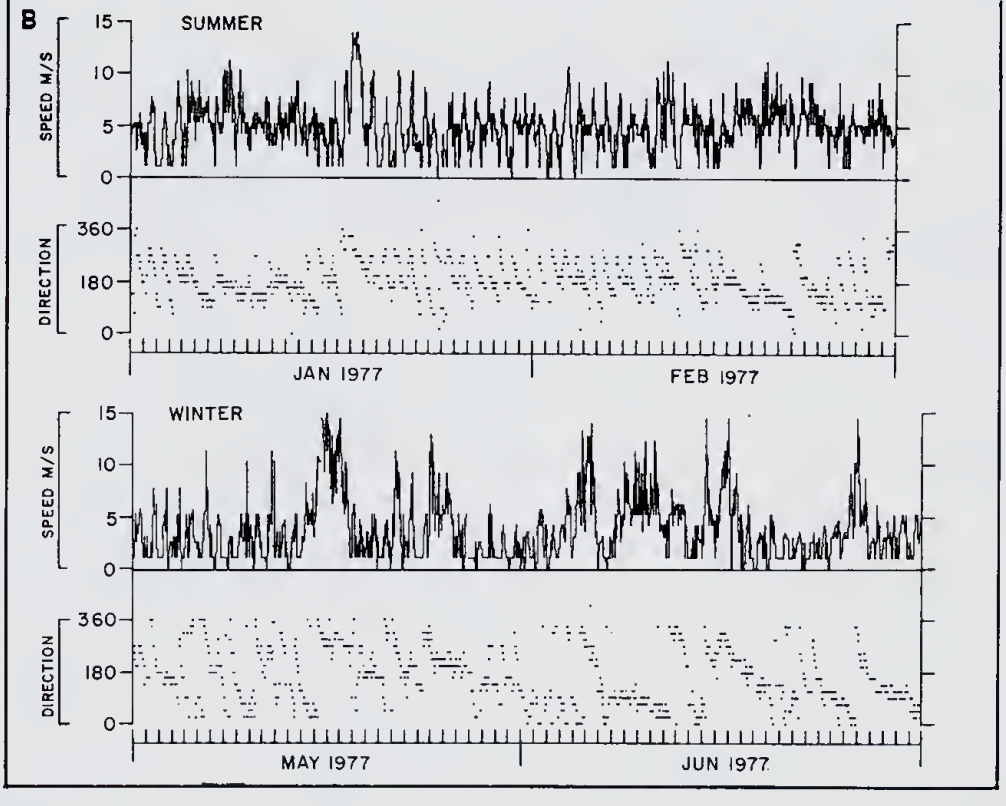

Figure 2.—A.—Bathymetric profiles of the submarine shelf along transects 4, 5 and 6 (see Fig. 1 for location). B.—Examples of the pattern of variation of wind speeds and direction (10 m above surface) during summer and winter, typical of the Bunbury area.

Figure 3.—A.—Map showing geomorphic elements of the hinterland and Leschenault Inlet. B.—Bathymetric profile across transect 1. C.—Summary of the range of soils and shallow stratigraphy representative of each of the geomorphic sub-units in map A.

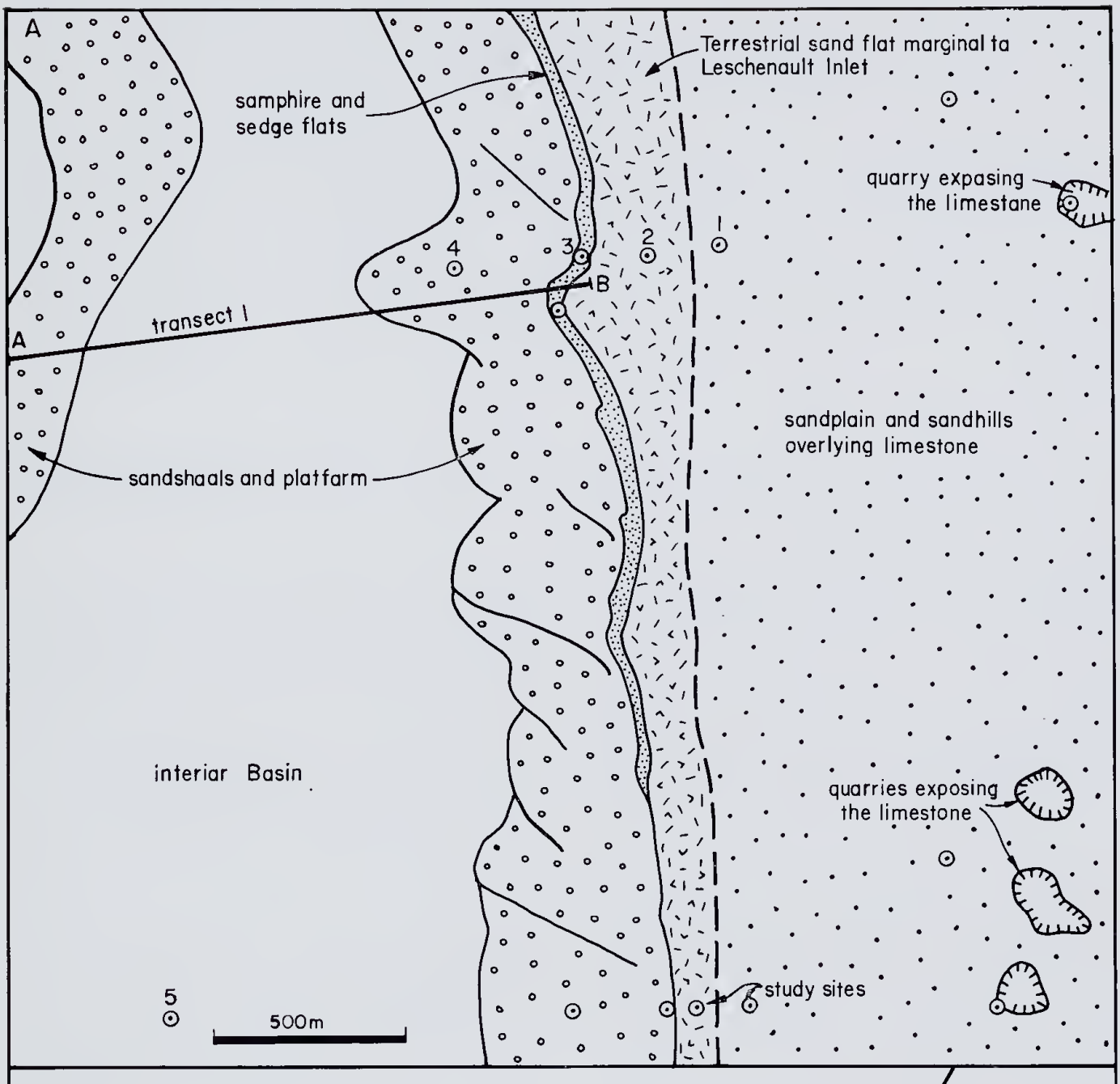

B. PROFILE ACROSS A-B

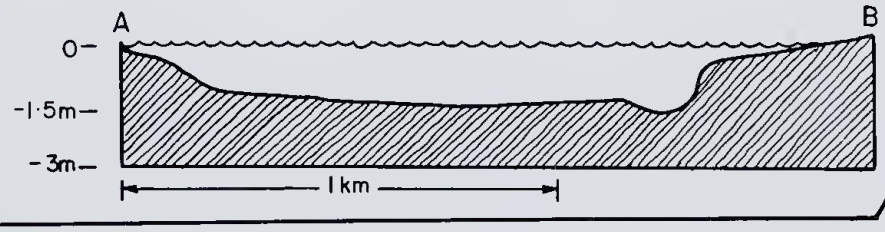

C. SHALLOW STRATIGRAPHY & SOILS AT LOCALITIES 1-5

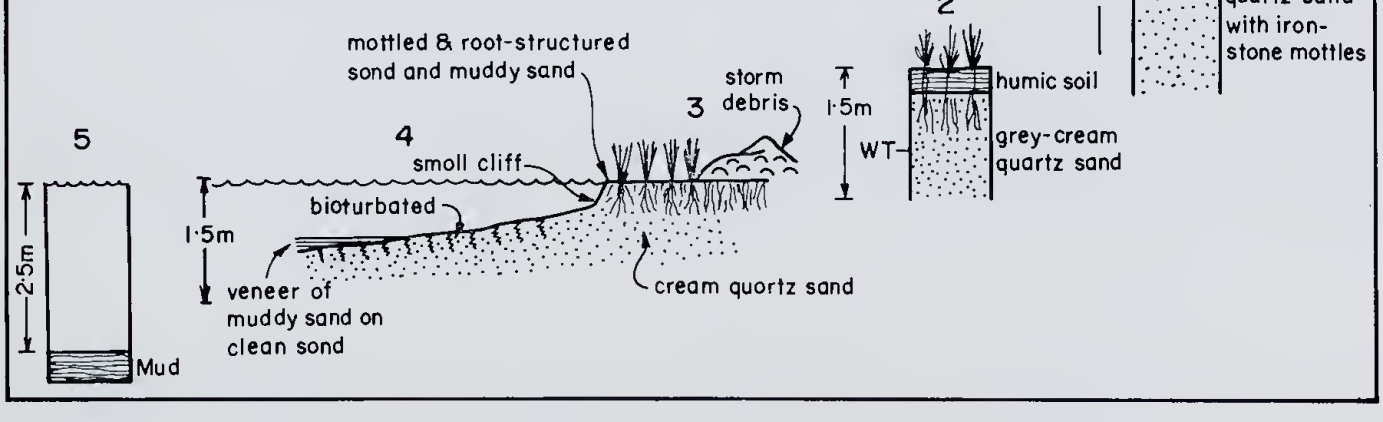

Table 3

Predicted locally wind-generated wave heights by direction using the 1977 Bunbury Power Station wind records. The body of the table shows relative frequency as a percentage (rounded to nearest 0·1%).

Direction (Deg.)	Significant wave height in metres †								
	0·0–0·2	0·2–0·4	0·4–0·6	0·6–0·8	0·8–1·0	1·0–1·2	1·2–1·4	1·4–1·6	1·6–1·8
338–22	0·3	0·7	0·1	0·1	*	....	....	....	....
23–67....	3·1	1·1	0·1	*	*	....	....	....	....
68–112	9·3	0·5	*	....	*	....	....	....	*
113–157	13·0	5·8	0·3	....	....	....	....	....	....
158–202	8·0	6·2	4·3	1·4	0·6	0·3	0·1	*	....
203–247	3·2	1·7	1·9	2·2	0·1	0·7	0·2	0·3	0·1
248–292	1·4	0·9	2·2	4·3	0·4	2·2	0·6	1·0	0·7
293–337	0·9	0·8	1·3	2·1	0·1	1·3	0·4	0·6	0·6

The matrix was computed by R. K. Steedman and Associates using the SMB Method. This is a procedure developed by Sverdrup and Munk (1947) and modified with additional empirical data by Bretschneider (1959). Wave data generated for a water depth of 10m. The matrix does not include the persistent westerly and south-westerly swell that arrives in the area from storms in the southern Indian Ocean.

* denotes occurrence is $<0{\cdot}05\%$.

† Wave height in group 0·2–0·4 implies $0{\cdot}2 <$ wave height $\leq 0{\cdot}4$, etc.

breezes. As a result there is a net mobilisation of the dry sand of the beach and dunes from the west to east across the peninsula. Figure 2B also shows a large proportion of sand-shifting wind occurs in summer. During winter there is a less frequent occurrence of sand-shifting wind, near ground level; those that do occur come from the south-west to north-west quarters; however the unconsolidated beach sands and mobile dunes of the peninsula tend to be damp and are therefore less prone to mobilisation by wind.

Oceanography

The Leschenault Peninsula is bounded by the Indian Ocean. However, the seafloor in this region is shallow for a substantial distance offshore (Figure 2A). As a result the wave and swell regime is markedly attenuated on reaching the beach; during storm conditions, the wave regime is further modified by a series of reefs lying close and parallel to the existing shorcline. The predominant forces of the wave regime along the coast are due to the combination of swell and wind/wave. The net transport of beach sediment is dependent largely upon the orientation of wave attack. Table 3 summarises data on significant wave height generated by wind. This shows the predominant wind waves that impinge on the coast are from the west and south-west sectors. When these are combined with the predominantly west and south-west swell there is a net northward movement of sediment in the shore zone.

An important element in the erosion of this beach is astronomical and storm tidal levels. The Bunbury region has a very small tidal amplitude (Hodgkin and Dilollo 1957). The tides are diurnal and have the following ranges (Australian National Tide Tables 1979):

Highest astronomical tide (HAT)	+ 1.3 m
Mean higher high water (MHHW)	+ 0.9 m
Mean sea level (MSL)	+ 0.6 m
Mean lower low water (MLLW)	+ 0.4 m
Lowest astronomical tide (LAT)	0.0 m

However mean sea level is influenced markedly by barometric pressure. During summer the area is dominated by high pressure systems which give way to low pressure systems during winter. As a result, there is a general shift in mean sea level of up to 0.5 m between winter and summer. During winter storms, the low pressure accompanying storms together with wind stress on the sea toward the coast combine to ensure that storm wave attack tends to be high up the beach. Net erosion, however, can have an irregular pattern from year to year. Consequently there are a number of seasons with only minor erosion and in occasional years, with intense erosion.

Leschenault Inlet is a shallow elongated lagoon with water depth less than 2 m. Wave energy within Leschenault Inlet is due entirely to local wind waves. During summer wind waves generated by the sea breeze are sufficient to suspend muds from the shallow floor of the inlet.

The hydrologic characteristics of the water within Leschenault Inlet have changed recently. Prior to 1951 the entrance of Leschenault Inlet to the sea was at the southern end of Koombana Bay. Both the Collie and the Preston Rivers entered Leschenault Inlet and, together with substantial drainage from the north, they exerted a fresh water influence at the end of winter. As a result, the general characteristic of Leschenault Inlet was brackish during winter and marine during summer (Rochford 1951, Meagher 1971). After making an artificial entrance (referred to locally as "The Cut", Fig. 1) to the lagoon adjacent to the two rivers, the hydrology changed virtually to that of a marine embayment. Brackish water influences now are much reduced and the inlet remains essentially marine in salinity throughout much of the year other than for the occasional outflow conditions from the Collie and Preston rivers. The outflow from the Collie River also has been substantially reduced as a result of the catchment upstream.

There was a far higher incidence of flooding over the surrounding land along the eastern foreshores of Leschenault Inlet prior to the development of the Bunbury region (with the consequent impounding of water from the Collie River and the artificial channel cut through the lagoon). Thus geomorphic influences have been substantially changed within the last 100 years. The higher incidence of flooding and the retention of water in low-lying areas further into summer, could be expected to influence not only the aquatic vegetation and fauna of Leschenault Inlet but also the strandline vegetation and sediments peripheral to the inlet.

1·8–2·0	2·0–2·2	2·2–2·4	2·4–2·6	2·6–2·8	2·8–3·0	3·0–3·2	3·2–3·4	3·4–3·6	3·6–3·8	3·8–4·0	4·0–+
....	....	....	....	....	....	....	....	....	....	....	....
....	....	....	....	....	....	....	....	....	....	....	....
....	....	....	....	....	....	....	....	....	....	....	....
....	....	....	....	....	....	....	....	....	....	....	....
....	....	....	....	....	....	....	....	....	....	....	....
*	0·2	0·1	....	*	....	....	*	....	....	....	....
0·1	0·8	0·8	0·1	0·2	*	0·1	0·2	0·1	0·1	0·1	0·2
0·1	0·8	0·5	*	0·3	*	0·1	0·2	0·1	*	0·1	0·2

No. of data points = 8 744
Mean wave height = 0·5
Maximum wave height = 5·4
Standard deviation = 0·7
Percentage calm = 2·8

Geomorphic units

The study area is located toward the southern end of the Swan Coastal belt (Jutson 1950, Gentilli and Fairbridge 1951). Most of the land surface of this area is composed of sediments of Pleistocene to Holocene age which have been deposited in a range of marine, fluviatile, lacustrine and aeolian environments (Seddon 1972).

In the immediate vicinity of Leschenault Inlet there are 4 major geomorphic units based on the criteria of physiography, sedimentary materials and biological habitat. From east to west these are (Fig. 1): (1) hinterland, (2) inlet, (3) peninsula and (4) submarine shelf.

Within the peninsula and inlet units, sedimentation is still continuing. As a result there are modern analogues of much of the material examined in excavation, cliffs and in cores. The ocean shore portions of the peninsula and the submarine shelf are in a predominantly erosional phase. Many geological features of the nearshore area are the result of a retreating coast and an exhumed old surface (unconformity).

Hinterland

Hinterland is a convenient term used here to describe the aggregate of land units (Spearwood, Bassendean, and Blythewood units; McArthur and Bettenay 1960) to the east of Leschenault Inlet. The land surface is undulating with average relief generally less than 20 m; some local areas have relief up to 30 m above sea level. The hinterland is covered by a variety of soils (McArthur and Bettenay 1960). Each of these has a recognisable vegetation assemblage (Seddon 1972). In broad terms, these vegetation assemblages range from *Eucalyptus* and *Banksia* forests and woodlands in the higher areas (where they have not been cleared for agriculture) and *Melaleuca* wetlands in the lower areas.

Figure 3 shows the distribution of sedimentary materials adjacent to the foreshore of Leschenault Inlet. The main sedimentary materials are: Tamala Limestone (Playford *et al* 1976)—Spearwood Dune System (McArthur and Bettenay 1960), (2) Quartz sands overlying the Spearwood Dune System and Bassendean Dune System (McArthur and Bettenay 1960) and (3) Fluviatile, lagoon and deltaic sediments—Vasse and Blythewood Systems (McArthur and Bettenay 1960).

Inlet

The Leschenault Inlet is a lagoon some 14 km long, between 1.5 km and 2.5 km in width and 0.3 m to 2 m in depth which lies parallel to the coast and is separated from the Indian Ocean by a narrow barrier. It can be subdivided into 3 geomorphic sub-units; these are sedimentologically and biologically distinct and can be related readily to depth of water. The sub-units are (Fig. 3): (1) samphire and sedge flats, (2) sand shoals and platforms and (3) interior basin.

Samphire and sedge flats. Strandline flats, inundated by high-tide and stormwater level, are covered by vegetation such as samphires *Arthrocnemum bidens* and *Suaeda australis* and the sedge *Juncus*. Shoreline trees such as *Melaleuca raphiophylla, M. cuticularis, Casuarina obesa,* and the mangrove *Avicennia marina* occur in scattered and individual copses.

Sediments underlying the surface of this zone are variable; mostly they are root-structured muds, or muds burrowed with sand/mud mixtures and organic detritus. Locally substrates are predominantly sand. Sediments are grey to black due to organic detritus and iron sulphide. Along the eastern shoreline there are local ribbon and shoe-string deposits (5-30 mm thick) of shelly gravel, coarse sand and organic detritus. They have formed by shoreward transport and accumulation of sedimentary materials during storms (Fig. 4C) which are accompanied by elevated water levels and strong wind waves.

Sand shoals and platforms. Shallow sand shoals and platforms occur along both sides of the inlet (Figs. 3, 5) between MHHW and 0.2 m below MLLW. They become (partially) exposed during a combination of low tide and high barometric pressure.

Shoals are the subaqueous terminal portions of sand dunes that extend into Leschenault Inlet. On the western side they are due to the progradation of the mobile dunes; on the eastern side they are due to the encroachment of the inlet on the old dunes of Pleistocene age. Reworking and mobilisation by currents and waves results in cusps and spits along the shoreline at the tip of shoals.


A


B


C

Platforms are narrow units that border the remaining coastline of the inlet; their margins are straight, gently curved or lobate. Platforms originate as wave-built and current-modified features formed from sediment eroded off dunes and sandhills adjoining the inlet. Sediments of shoals and platforms are derived from quartz calcareous sands on the west margin, and from siliceous sands on the east margin of the inlet.

Vegetation on sand shoals and platforms consists of a number of unattached and semi-attached algae together with the seagrasses *Zostera* and *Halophila*. The top layers of sediment are well bioturbated by a range of crustaceans, worms and fish. Mollusc fauna of the platforms contribute shells to the sands. Mud layers that accumulate on the surface during quiescent periods are mixed into the sediment by

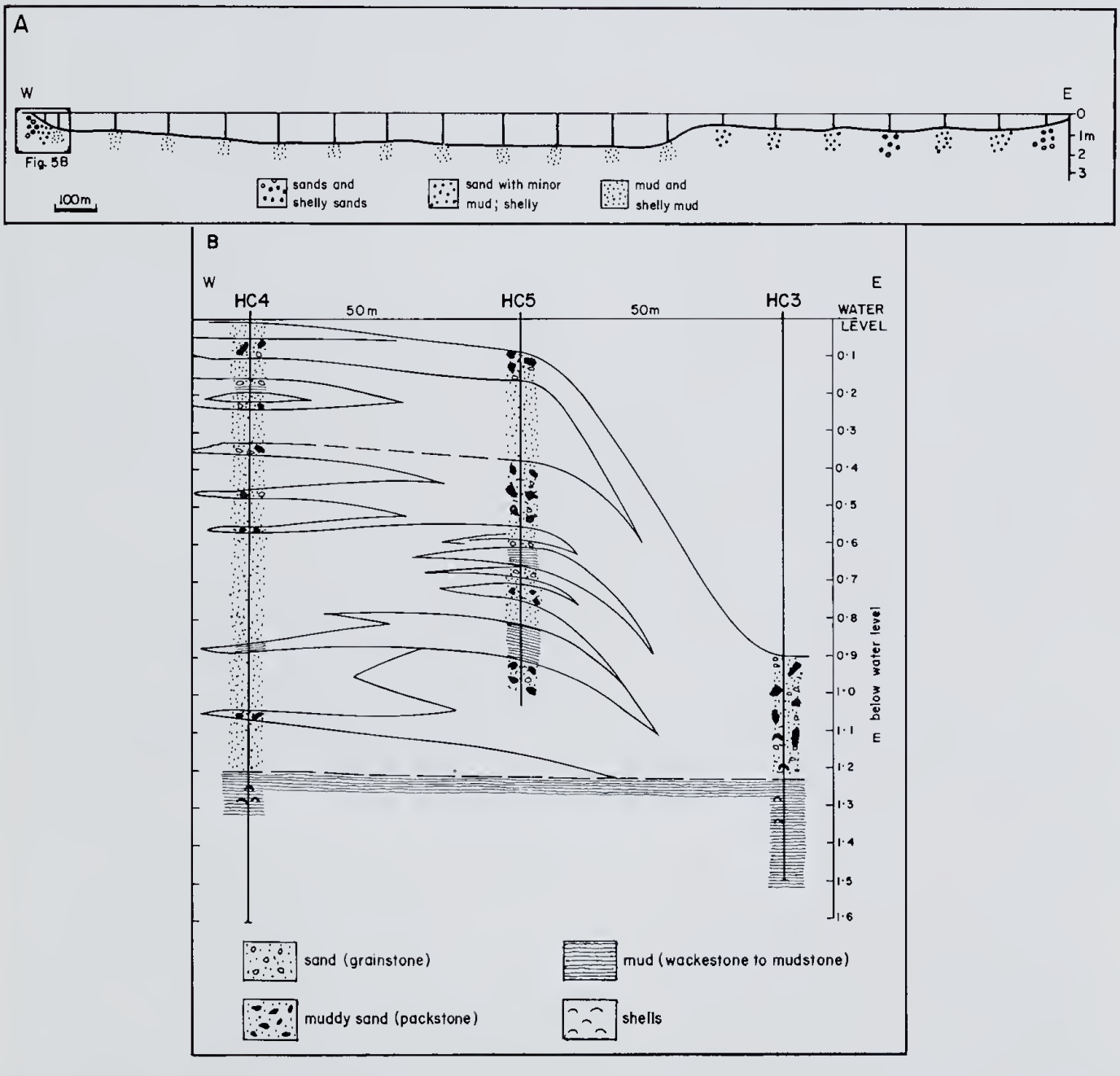

Figure 5.—A.—Bathymetric profile and surface sediment types along transect 2 (see Fig. 1) across Leschenault Inlet. Shoals and platforms on the shallow margins are composed of sand and muddy sand; the deeper interior basin is floored by mud. B.—Detail of inset. The profile illustrates the variability of shallow stratigraphy within a shoal. Water level is MSL.

Figure 4.—A.—Aerial view of Leschenault Peninsula. Its seaward edge is clearly marked by the narrow ribbon of orange-stained beach and beach ridge sands (light grey on photograph); these abruptly adjoin the white sands of the eroding dune line. The bulk of the Peninsula is composed of bare and mobile dunes interspersed with vegetated dunes. B.—Advancing front of a mobile dune, here encroaching upon a heath-covered dune. The mobile dune is an attenuated parabolic form which appears as an east-west elongated finger of sand. The location of this dune is shown arrowed on Figure 6. C.—Strandline storm deposits of sand, shell and vegetation debris tossed up onto the sedge and samphire flat along the margin of Leschenault Inlet.

burrowing organisms. Thus, depending on intensity of biological activity and rate of mud influx, the sand shoal and platform areas have varying proportions of shelly sand, muddy sand and burrowed clean sand.

Interior basin. At the edge of a shoal or a platform there is often a marked slope (Figs. 3, 5) which falls from 0.2 m to 1.0 m below MLLW into the interior basin (maximum 3 m deep). The basin floor is dark grey to brown mud and some muddy sand. Resident animals contribute shells and burrow the sediment so that bioturbated, shelly muds are developed locally.

Relationships. Leschenault Inlet is quite obviously filling with sediment. Sand derived from margins extends into the inlet interfingering with, and prograding over, muddy sediments. The continuing *in situ* yield of seagrass and algae contributes humic material. The associated mollusc fauna contributes calcium carbonate debris.

Wave action and littoral drift along the inlet result in accumulation of muds on the shallow flats. Mud is commonly deposited on the western shore as a veener on sand. Mud is winnowed off the eastern sand platforms each day when the sea breeze generates small waves and induces long-shore drift. Some of this mud finds its way into the interior basin, but a significant amount of mud also is transported northwards and accumulates in a thick wedge along the northern inlet margin. There are 4 sources of mud: (1) rivers that drain into the embayment, (2) erosion of older, muddy estuarine deposits, (3) fine-grained organic detritus derived from breakdown of aquatic plants and (4) skeletal silt generated within Leschenault Inlet.

Typical transects across a shoal into the interior basin are illustrated in Figures 3 and 5. The shoals have prograded over mud floors which consistently occur at about 1.0-1.5 m below MLLW.

Peninsula

The peninsula separates the inlet from the sea and is an elongated barrier some 12 km long and between 0.8 km and 1.5 km in width (Fig. 4A). Its surface is undulating and consists of a series of vegetated and mobile sand dunes whose elevation ranges from near sea level to 40 m. These dunes have been assigned to the Quindalup system by McArthur and Bettenay (1960).

Beach sands occur along the western side of the peninsula and pass inland into bare exposed dunes. Vegetated dunes become more common toward the east. Along the eastern side of the peninsula, there is low-lying, flat land which has a cover of humic soil and coastal vegetation interspersed with vegetated dunes and mobile dunes. In some areas mobile dunes extend as tongues of sand into Leschenault Inlet.

Photographs taken during the 1940s, show that although some individual dunes have migrated significantly to the east, the distribution of dunes and vegetation along the peninsula is broadly the same as today. The photographs also indicate that this landform has been a natural peninsula which extended down the western margin of the inlet to its narrow entrance to Koombana Bay.

The Leschenault Peninsula is readily separated into 4 geomorphic sub-units:—(1) beach and beach ridge, (2) mobile dunes, (3) vegetated dunes and (4) woodland plain.

Beach and beach ridge. This zone encompasses both the beach-face and the supra-tidal storm ridge accumulations (Figs. 4A, 6). Sand, lithoclast gravel and shells comprise the beach and beach ridge sediment (Fig. 7A). The source of the material is local (derived directly from eroding dunes), nearshore (rocks, shells and sand from adjoining reefs) and offshore (coarse sand, shells, mud clasts and rocks). Waves and long-shore currents dominate the physical environment. As a result, sediments are laminated and cross-laminated. The mobile, shore sands have been artificially stained orange by iron within the last decade by factory effluent from processing of titanium minerals. Consequently the abrupt contact of the youngest beach/beach ridge sediments with both older beach/beach ridge sediments and other units is well marked (Figures 4A and 7B).

Mobile dunes. Parabolic mobile dunes comprise about 30% of the peninsula area. The dunes occur as elongate east-west fingers of sand that are interspersed with vegetated and partially vegetated dunes (Figs. 4A, 6). Movement is effected by the strong onshore winds. The dunes begin as parabolic blow-outs on vegetated older dunes. These older dunes contain abundant *in situ* calcified root casts and cemented laminae. As sand is mobilised, surface lags of the calcified casts and limestone plates (cemented laminae) form (Fig. 8D); these undergo later solution and disintegration by rainwater and the $CaCO_3$ is redistributed. The advancing eastern edge of mobile dunes progressively engulfs the established heaths, forests and woodlands (Fig. 4B) and buries the soil sheet upon which this vegetation grows (Figs. 8A, 8B, 9).

The internal structure of migrating dunes contains large scale cross-bedding and cross-lamination (Fig. 8D). The sediment of dunes is medium and fine sand (mostly quartz and calcareous components). There is compositional and textural variation at the scale of dunes and at the scale of laminae. The $CaCO_3$ content of individual samples varies from $< 1\%$ to 30% reflecting the variable composition of source material and the variable history of a dune. For instance, a dune with 5% $CaCO_3$ may overlie or be juxtaposed against a dune with 10-15% $CaCO_3$. There is similar wide variation in grain size and composition of laminae, which may be fine sand alternating with medium sand, or fine/medium sand mixtures alternating with medium sand; coarse sand and (thin shell) granule laminae also occur.

In the Leschenault study area, there is a large range of particles (differing in size, shape, composition and internal texture) that become exposed to enable mobilisation by wind (Table 4). The wind conditions which produce mobilisation are relatively consistent for a considerable period (e.g. south-west afternoon sea breeze through summer) and deposition of material is selective according to the combination of particle aerodynamics and the differential wind field across the dune. It follows that dune laminae deposited under consistent wind conditions are texturally and compositionally varied, depending on source and availability of sand grains. Variation in wind strength and direction produces grain size, as well as compositional, variation.

Vegetated dunes. Vegetated dunes are similar in external geometry, internal structure and sediment variation to mobile dunes. They develop when mobile

Table 4

Particle types composing the dune sands.

Grain size	Typical grain composition and shape
Very fine sand	Ilmenite and rutile grains, equant shape
Fine and medium sand	Quartz grains, equant shape. Solid $CaCO_3$ grains, equant shape (e.g. lithoclast, fragments of molluscs and urchins). Porous $CaCO_3$ grains, prolate shape (e.g. calcareous algae segments). Porous $CaCO_3$ grains, equant shape (e.g. foraminifers).
Coarse sand	Quartz grains, equant shape. Solid $CaCO_3$ grains, bladed shape (e.g. mollusc fragments). Porous $CaCO_3$ grains, prolate shape (e.g. calcareous algae segments).
Granule	Solid $CaCO_3$ grain, bladed shape (e.g. mollusc fragments).

dunes become progressively fixed by heath plants, (*Acacia, Anthroceris, Rhagodia*, etc.). A surficial sheet of soil develops under plant cover and, in time, dunes degrade to more gentle slopes. Surface soils become thicker (0.3-1 m), less calcareous, and mature in terms of organic content. The more soluble soil components (carbonate) are redistributed. Root systems (live and calcified) pervade the sands; calcified root structures become more abundant at depth.

The vegetation assemblage on the dune then matures. *Acacia-Anthroceris-Rhagodia* heath tends to remain on the exposed areas, hill crests and northern side of the dunes. *Agonis* (peppermint) forests tend to develop on the southern sides and in the hollows. The inter-dunal hollows preferentially accumulate humic material and develop characteristic thicker soil.

Woodland plain. This is a relatively flat surface typically covered by discrete groves comprised of tuart (*Eucalyptus gomphocephala*), peppermint (*Agonis flexuosa*), tuart/peppermint or *Acacia*. The plain is underlain by a soil (0.3-2 m thick) which overlies either a thin profile (2-3 m) of degraded dune sand or a calcrete sheet.

Alteration of sediments. There are several physical, chemical and biological processes that rapidly alter sediments in the surface and subsurface after deposition. The most obvious alteration products of the processes are soils, calcrete and sparry calcite cementation.

The soils of the peninsula, although volumetrically minor, are structurally and geomorphically important. Structurally because they are linked with and influence the groundwater regime; geomorphically because they indicate buried older heath-covered dune surfaces and woodland-covered plains (Fig. 9). The soils, humic calcaric regosols (Bridges 1970), are sands with a high humus content and are equivalent to the Ucl. 1 soils of Australian soil scientists (Northcote *et al.* 1975). They are forming today as 1-2 m

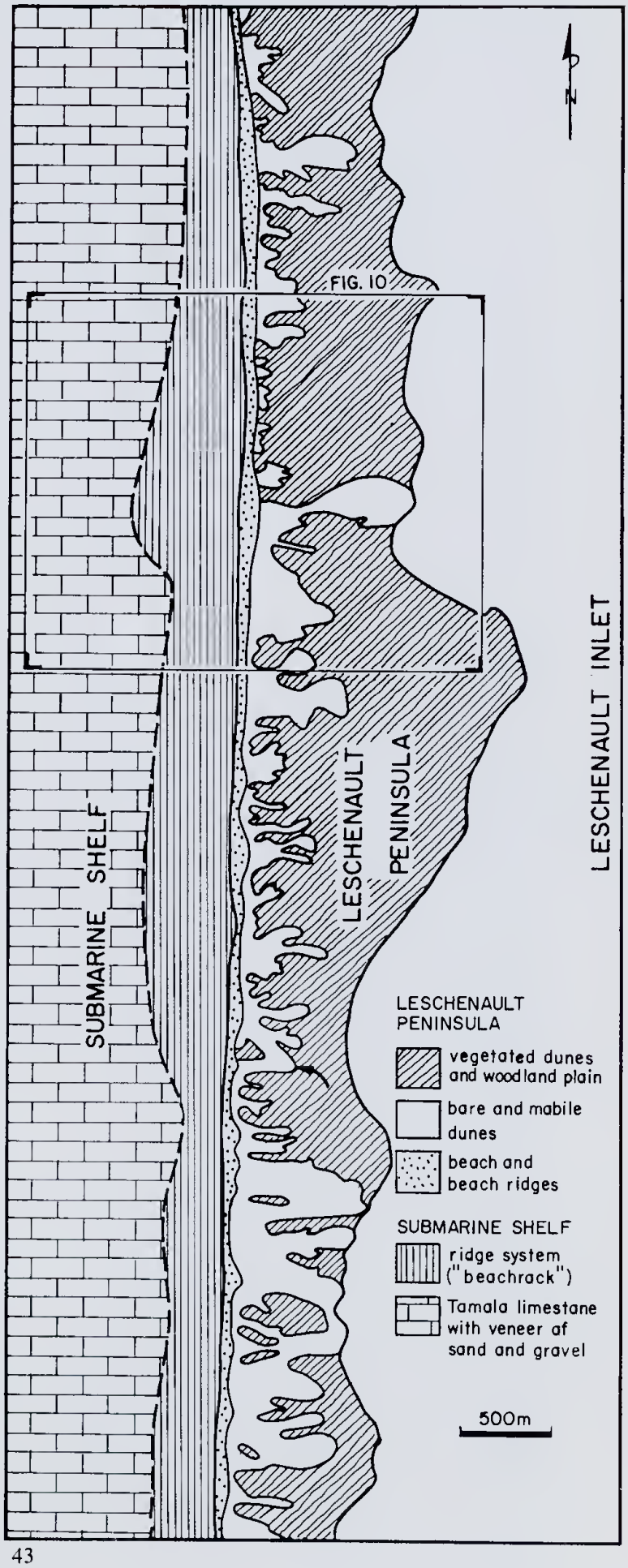

Figure 6.—Map showing geomorphic elements of the Leschenault Peninsula and the submarine shelf. Location of this area is shown in Figure 1. The arrow shows location of the dune illustrated in Figure 4B.

(3)—11558

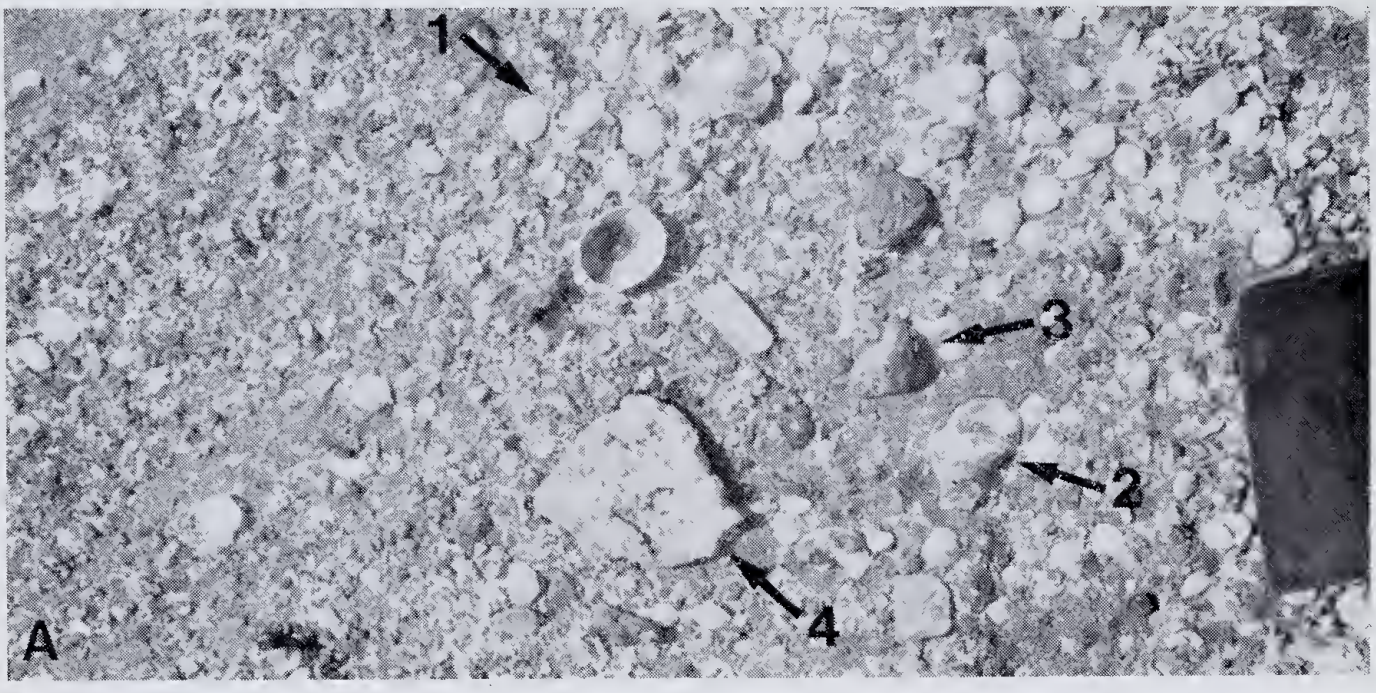

Figure 7.—A.—Surface gravel on beach face illustrating the range of gravel types. 1, recent nearshore bivalve, 2, estuarine oyster reworked from offshore mud outcrops, 3, platy limestone fragment reworked from offshore limestone reefs, 4, rounded basalt pebble. B.—Internal structure (cross-stratification) of beach ridge exposed by storm erosion following Cyclone Alby. The sharp contact between (young) orange-stained sand and (older) white sand within the beach ridge is outlined.

sheet veneers over dune sand. When buried by successive mobile dunes the soils appear in profile as undulating and bifurcating thin sheets which separate dune units. (Fig. 9).

There are 3 intergradational types of soil: (1) Dark grey humic quartz sand, which is humus rich, strongly root-structured and leached of its carbonate content. With depth it grades to a humic-rich quartz calcareous sand and then into a cream to light yellow quartz calcareous parent sand. This soil is typical of densely vegetated dunes and woodland plains. (2) Light grey to brown-grey quartz sand which is humus-poor (i.e. immature), and moderately to weakly root-structured. This soil forms on the surface of a fixed dune that supports heath vegetation.

Figure 8.—A.—Photograph showing old tuart forest on soil 3 (see Figure 10); these stumps and trunks have been exhumed by wind erosion. B.—Stratigraphy exposed in the wall of "The Cut" (Fig. 1). Trunks of tuarts and peppermints (arrow 2) are *in situ* on a soil sheet (up to 1 m thick) which is encompassed by the interval marked 1. C.—Coastal erosion following Cyclone Alby had cut back the dune line exposing stratigraphic relationships. The white sand of the old dunes is arrowed 1. Orange-stained beach ridges (arrow 2), which were developed in interdune depressions, also were truncated by the coastal erosion. The calcrete sheet (arrow 3) had been exhumed, cliffed and broken in to large blocks by the storm. D.—Dune cross-stratification exposed in a costean. Arrows 1 indicate cementation along laminae which now stand out in relief. The natural wind-deflated surface is littered with a lag of limestone plates (arrow 2) derived from these cemented laminae.

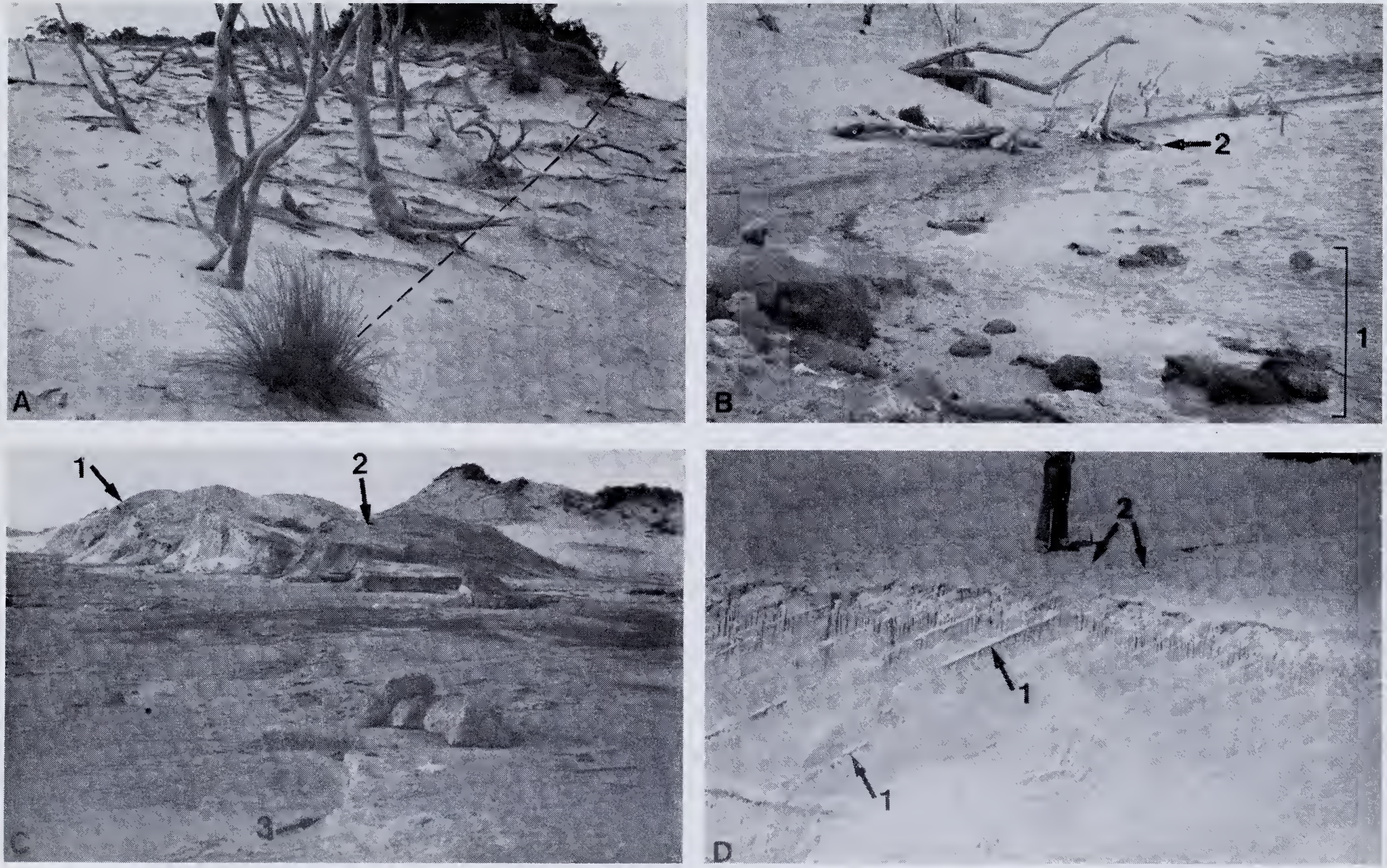
A
B
2
1
C
1
2
3
D
2
1
1

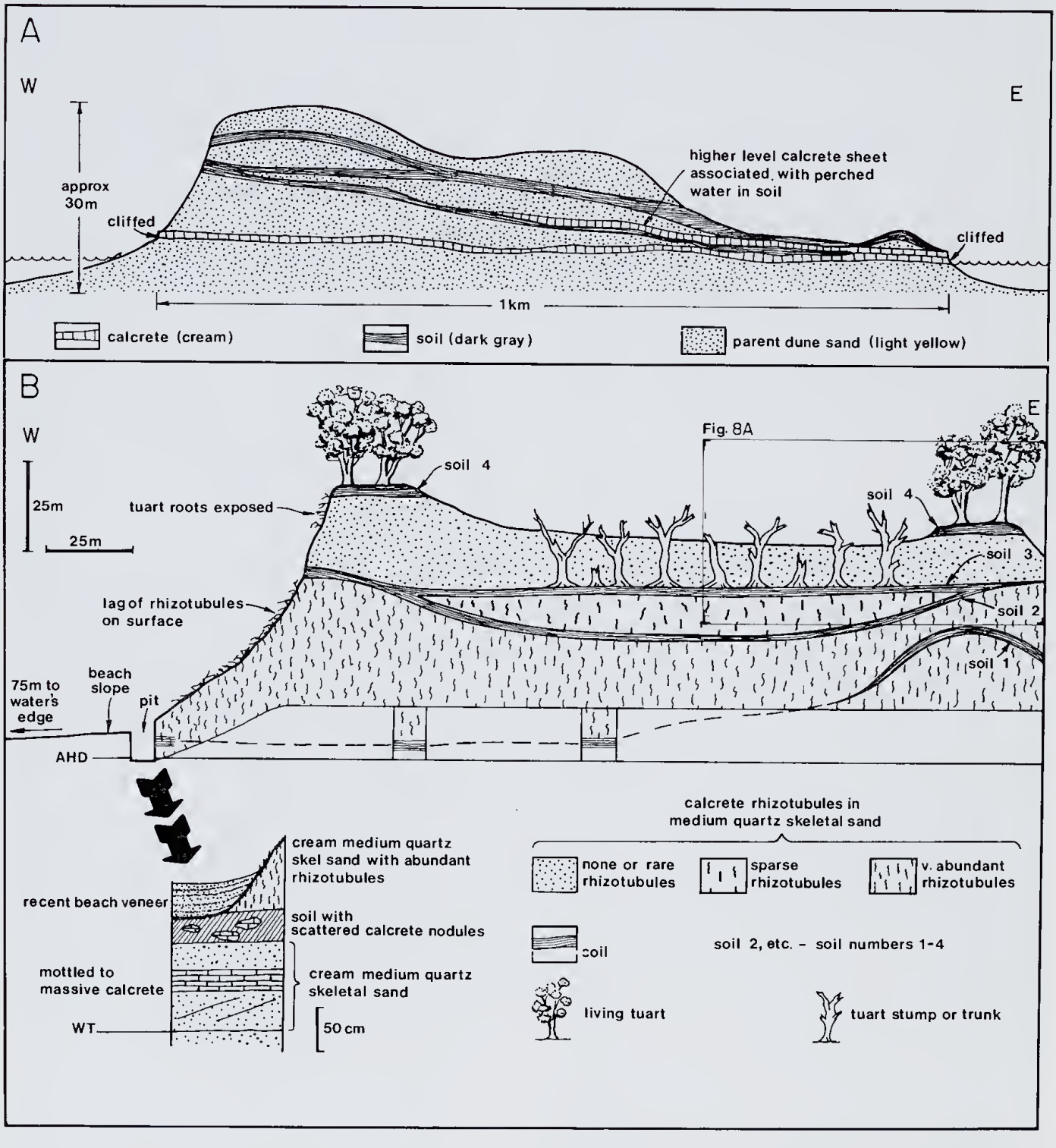

Figure 9.—A.—Diagramatic representation of stratigraphic relationships of dune sand, soils and calcrete across Leschenault Peninsula. B.—Profile along transect 3 (Fig. 1) illustrating shallow stratigraphy. Bifurcating soils separate various dune sand bodies. A fossil tuart forest is *in situ* on soil 3. The entire stratigraphic interval is cliffed to seaward. Wind erosion has sculptured the surface above the beach face; wave (storm) erosion has truncated the sequence at the level of the pit, and beach sands overlie the erosional surface.

(3) Brown-grey calcareous quartz sand with little humus content; it is moderately to weakly root-structured and occurs where inblown sand has diluted the humus contribution. This soil forms under cover of sparse vegetation on recently fixed dunes.

Calcrete is a fine-grained aggregate of $CaCO_3$ developed as a thin widespread sheet above the water table (specifically in the upper capillary zone). It forms under the dunes by evapo-transpiration. The calcrete has a number of structural forms (mottled,

massive, laminar) that reflect stages in its development. The calcrete sheet is truncated by marine erosion, and occurs cliffed at the west margin of the peninsula (Figs 8, 9); on the east margin it is either cliffed or locally buried by mobile dunes (Fig. 9).

In the subsurface there also is local and patchy cementation of sand by *sparry (low magnesium) calcite* (Fig. 8D). At its maximum development about 30% of the profile may be cemented. The cementation is mostly incomplete, and crystals merely fringe and bind grains into coherent aggregates. The disposition of the cement results in selective induration of sand laminae. Most of the cementation has been observed in sand deep in the dune profile but above the present water table.

Relative age sequence in dunes. Cliff exposure and trenches indicate that cementation of sands is largely confined to older dunes low in the profile and it is on criteria of cementation, occurrence of calcified root casts (rhizotubules or rhizoconcretions) and calcrete that relative ages of sequences within the dunes are recognised. Modern dunes are uncemented and lack even calcified root casts. Older dunes contain a moderate amount of calcified root casts and are irregularly cemented in scattered patches (Fig. 9). The oldest dunes contain abundant calcified root casts and are irregularly cemented by calcrete and sparry calcite throughout much of their profile (Fig. 9). Older dunes and associated soil sheets are traceable to below present sea level indicating dune emplacement and soil formation before the Holocene sea reached its present level.

Submarine shelf

The submarine shelf is a gently sloping feature extending from low water to over 20 m depth (Fig. 2A). The sea floor directly offshore the peninsula in the study area is composed of 5 materials: (1) outcrop of Tamala Limestone, (2) beachrock, (3) estuarine mud, (4) unconsolidated sediment and (5) basalt.

Most of the sea floor in the kilometre adjacent to the study area of the peninsula (Figs. 6, 10) is formed of Tamala Limestone. It has been observed in this study to occur at depths of 18 m or more (some 8 km offshore). The general line of reef outcrops follows the general orientation of the present coastline (Fig. 6). Within 1 km of the shore, local knolls (reefs) protrude into shallow depths at random locations nearshore and along the beach. The submarine limestone topography varies from pavements to rugged reef. The pavement outcrops are veneered by sands through which limestone outcrop or reef (up to 2.0 m high) may protrude. In larger rocky reef outcrops karst and weathering features (such as caves, vugs, crevices, pinnacles, solution pipes and calcrete) are evident.

In an elongate area essentially parallel to the length of the peninsula and between low water and 6 m depth the shelf is dominated by ridges of "beachrock". The ridges, 1-4 m high and 100-300 m apart, are sub-parallel to the shore (Figs. 6, 10). Marine erosion is controlled by sedimentary structure and has resulted in a craggy slab-like to stepped surface morphology. Sand locally veneers these ridges but more commonly, forms shallow accumulations within inter-ridge depressions.

The ridges are composed of marine-indurated (cemented) sands, gravelly sands and shelly sand (informally termed "beachrock" in this study) that are similar to beach sediments onshore. The sediments are cemented by magnesian calcite crystals; in contrast, Tamala Limestone and the dune sands of the peninsula are cemented by low magnesium sparry calcite and calcrete. The cementation, that is quite marked in the submarine environment and in the phreatic marine zone under the beach face, occurs in a zone 3-4 m thick. Whilst the relics of former ridges of beachrock remain offshore and cementation is present beneath the beach, the zone of induration is not traceable to any extent under the peninsula. The beachrock cementation appears to have taken place in the phreatic zone under the beach face where outflowing fresh water and marine phreatic water adjoin (mix) and is similar to beachrock formation described from tropical regions (Bricker 1971).

The continuing coastal erosion along the beach face removes sands overlying newly formed beachrock and exposes the cemented zone. Progressive coastal erosion thus leaves in its wake, ridges and sheets of beachrock (Fig. 10). Newly exposed beachrock is subject to wave attack and biological erosion and, in time, is broken down. All stages of beachrock exhumation and disintegration are now evident along the nearshore area adjacent to the Leschenault Peninsula.

In local areas estuarine sediment (interlayered shelly mud and sand) occurs at levels of about – 1.5 m to – 8.0 m below AHD beneath the dune sands of the peninsula, as well as under Leschenault Inlet. In general, submarine outcrop is limited but there is an extensive (pavement) exposure offshore from "The Cut" (Fig. 1); the western margin of the outcrop is terminated by a cliff 0.5 m high.

Inshore, along the peninsula shoreface and flooring areas in depressions between ridges and rocky limestone knolls, are extensive but shallow, accumulations of unconsolidated sediment; these also locally veneer the top of rocky areas. The sediment is mainly sand, gravelly sand and shelly sand, that is bare and rippled or colonised by weed. Internally, this sediment is laminated and cross-laminated. Sources of sand are local (erosion of limestone and "beachrock" ridges), onshore (beach) and offshore. Shells are from encrusting communities on nearby rock reefs, and from resident animals in the sediments. Rock gravel is derived from the nearby limestone reefs and basalt outcrops. Locally, there are small accumulations of mud clasts and estuarine oysters recently reworked from estuarine muds that crop out on the sea floor.

Further south in the vicinity of Bunbury and its harbour the shelf is a relatively smooth flat pavement of fresh basalt and eroded weathered basalt covered locally by sand, gravel or mud.

Geomorphic processes

The major processes important to the development of the Holocene geomorphology and history of the area are sedimentation and erosion.

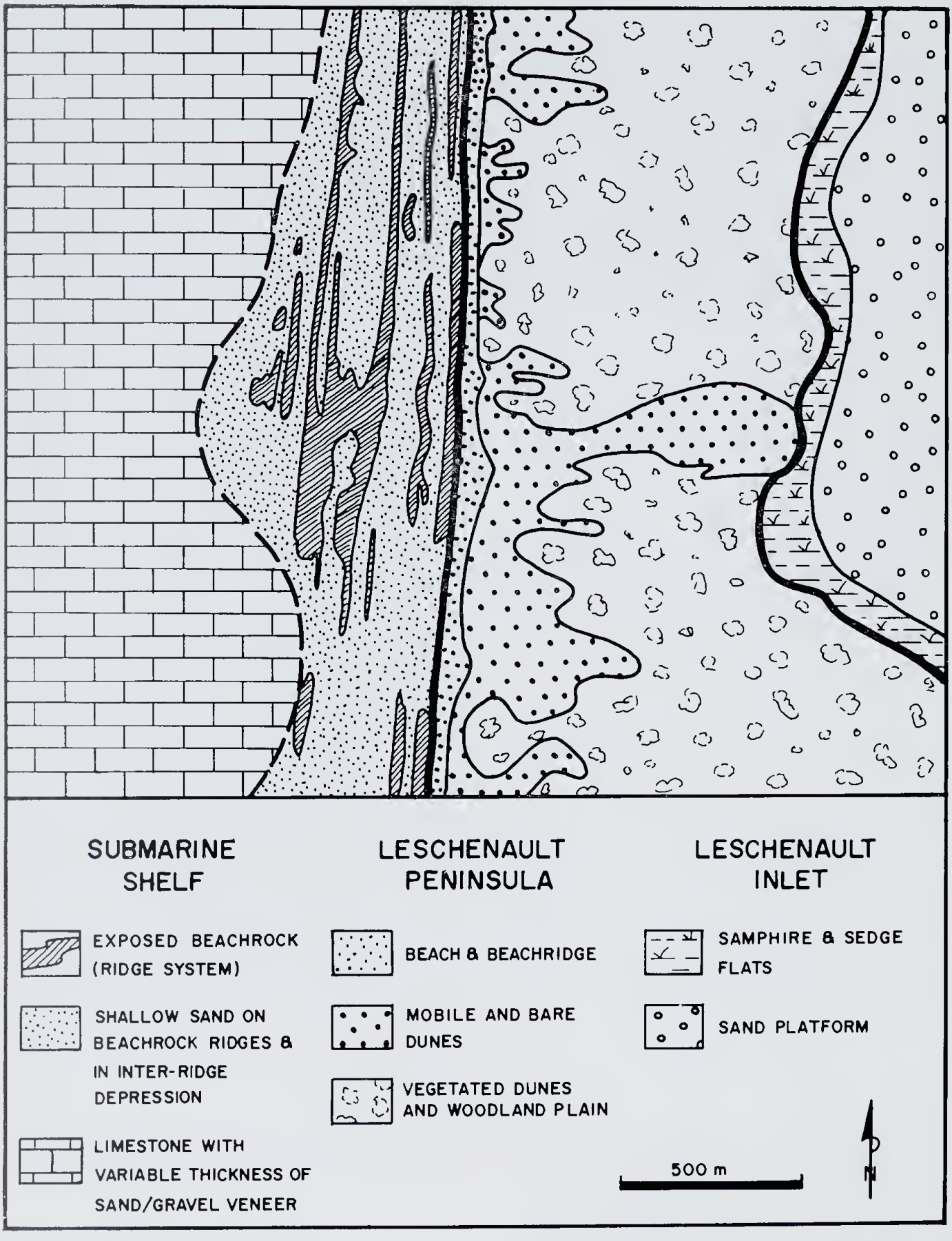

Figure 10.—Detailed map of geomorphic elements across submarine shelf, Leschenault Peninsula and Leschenault Inlet. Locality is shown as inset on Figure 6.

Figure 11.—Maps drawn from aerial photographs (A, 1941; B, 1971) illustrating extent of coastal erosion, dune encroachment and revegetation. Some of the more obvious changes are labelled.

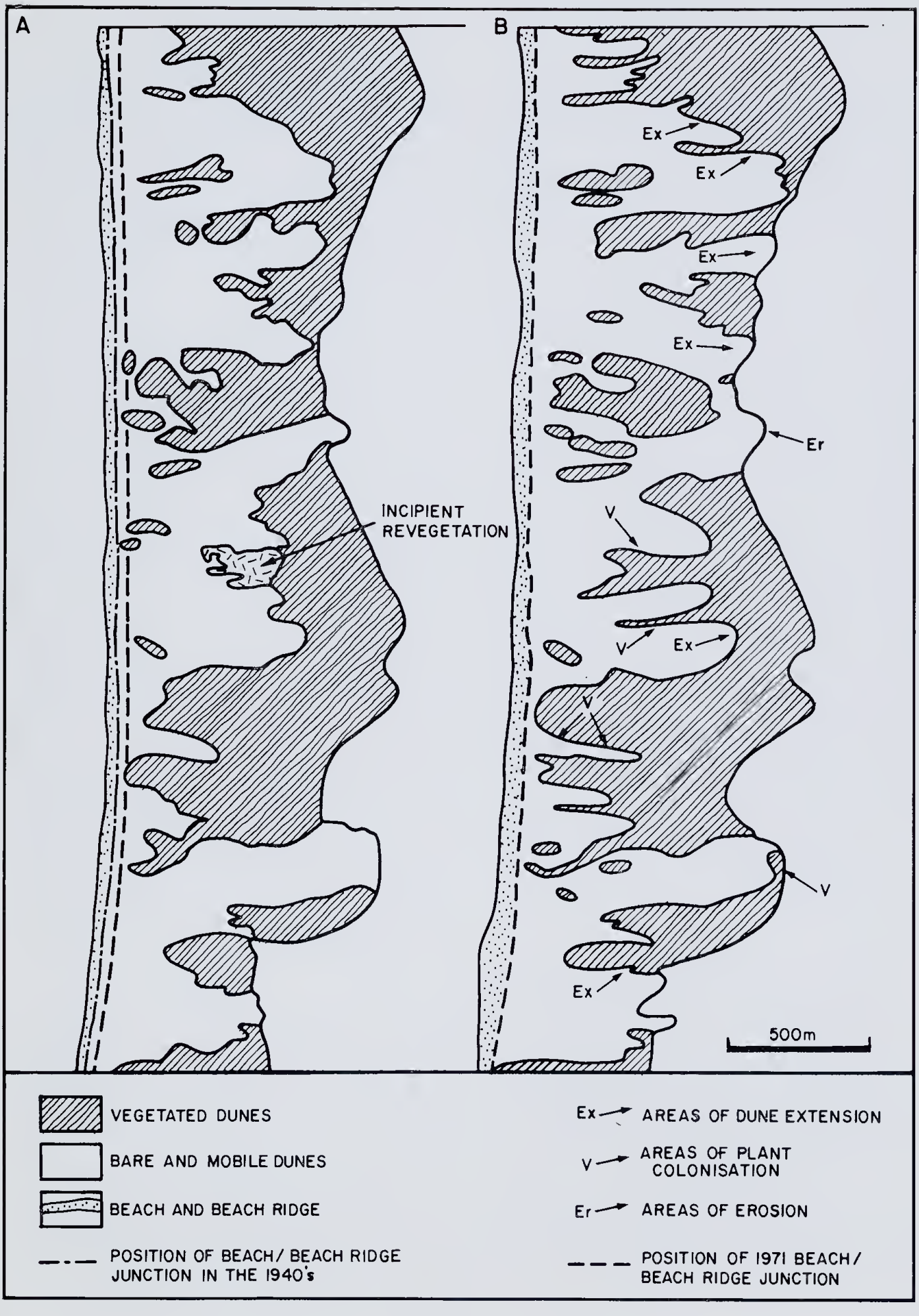
A
B
INCIPIENT
REVEGETATION
Ex
Ex
Ex
Ex
Er
V
V
Ex
V
V
Ex
500m
VEGETATED DUNES
BARE AND MOBILE DUNES
BEACH AND BEACH RIDGE
POSITION OF BEACH/ BEACH RIDGE JUNCTION IN THE 1940's
Ex AREAS OF DUNE EXTENSION
V AREAS OF PLANT COLONISATION
Er AREAS OF EROSION
POSITION OF 1971 BEACH/ BEACH RIDGE JUNCTION

Sedimentation

The main sedimentation sites are Leschenault Inlet, the peninsula dune system and the beach/beach ridge shoreface. Leschenault Inlet is filling with sand from (dune) margins, and with mud in the central portions. Sedimentation is more rapid on the peninsula where extensive mobile dunes are periodically developed. The mobile dunes extend as attenuated parabolic forms burying older dune topography. They ultimately spill into the inlet, contributing to shoals and platforms.

Examination of aerial photographs (between the 1940s and 1979) shows that 3 or 4 dunes in an area along some 3 km of peninsula significantly extended further eastward by 100-300 m over 30 years (Fig. 11). Blow-outs are initiated more frequently on the western wind-exposed shoreface. On-site study over 2 years indicates that some active dunes migrate at 3-10 m/year, a rate comparable with that derived from aerial photographs. The faster rates were encountered with dunes closer to the western shore. Dune migration is clearly staggered; dunes formerly mobile, are now fixed, and new blow-out sites are continually developing.

Sedimentation occurs on a seasonal basis on the beach shore. The beach face (foreshore and backshore) varies in width from 50 m in winter to $>$ 100 m in summer. The sediments are in definite stratigraphic sequence: subtidal, trough-bedded sands and gravelly sands, overlain by swash-zone, laminated sands, overlain by storm-level sands and shelly sands. The sediment suite forms a shore-fringing wedge or ribbon that is continually migrating to eastward as the coast erodes.

Beach-ridge sedimentation, in contrast, is localised in small hollows or embayments. There is little opportunity for beach ridges to form against a steep eroding cliff line, but in the larger interdune depressions (wind-eroded hollows) gradients are low and beach ridges develop. There is characteristic (1 m-sized) cross-stratification and a covering of vegetation (Fig. 7B).

In the context of retreating coastline, the existence of beach ridges in the hollows is temporary; coastal erosion ultimately incises them. New localities however are continually being exposed in which beach ridges can develop.

Erosion

Erosion is widespread and important on the western peninsula shore where it is a dominant factor in developing both the coastal morphology and submarine shelf. Elsewhere it is relatively minor and alternates with sedimentation. Two types of erosion predominate, wind erosion and wave erosion.

Wind erodes sand on the western face of the peninsula, continually exposing roots of living plants and leaving surface lags of cemented materials (Fig. 9). The effect of wind in this situation of limited sand supply from nearshore/offshore areas is slow, but the result is net erosion.

The foreshore along the Leschenault Peninsula changes seasonally from a full summer beach to a depleted winter beach. Periodic major storms and cyclones result in severe erosion. The vegetation line at the back of the beach is eroded (Fig. 8C) during those occasional storms that coincide with low barometric pressure and a correspondingly elevated mean sea level. During 1978 two such storms occurred. Coastal retreat of up to 30 m was recorded following the storm in March and Cyclone Alby in April. Water was elevated by 2 m and wave action cut into the toe of dunes collapsing the cliffs (Fig. 8). After these storms the beach was inspected before the fresh cliff face of sand collapsed. Although the beach is relatively consistent in alignment, the exposure showed that some new areas were exhumed (as indicated by a collapse of the protruding calcrete sheet Fig. 8C)). At other locations the storms had truncated beach-ridge debris which had been deposited and buried in the past 10 years (Fig. 7B). Thus, the two storms did not result in uniform erosion along the same coastline.

A review of the photographic record shows that whilst there are minor short term oscillations in beach line there has been overall net erosion of the beach face in the past 35 years (Fig. 11). Comparison between 1941 and 1971 aerial photographs shows that the coast suffered a net retreat of about 30 m; between 1971 and 1978 there was negligible erosion, however, in 1978 the coast retreated locally up to 30 m.

In summary, it is evident that coastal retreat is proceeding consistently and slowly by wind erosion, more moderately (1-2 m/year) by seasonal storms and winter waves, and rapidly but sporadically by periodic large storms and cyclones. The result is net erosion.

The influence of erosion on the coastal morphology is direct. Firstly, the entire western shoreface is steeply cliffed with exposures of roots and internal dune features (soils, laminae, cemented zones). Surficial sediments are stripped away and older stratigraphic units are exposed (Figs. 8, 9). For instance, calcrete and soils that crop out on the shore face are cliffed on a seasonal basis and eroded back by up to 1-2 m/year; these small cliffs are buried by the beach sediments in the following summer. Erosion of older sedimentary units contributes sand to the next sedimentation cycle. Secondly, as the coast retreats, it leaves in its wake, a newly exposed band of beachrock (Fig. 10). The net retreat is clearly reflected in the parallel bands of beachrock that form the submarine ridge system of the shelf. The extent of the beachrock indicates that at least 0.5 km of retreat has taken place leaving a vast expanse of cemented rock.

Discussion

Four major points of interest arise from this study. All of these have local implications for the Australind-Leschenault Inlet area, but some have more regional implication for the development of the Swan Coastal Plain. The first is that erosion is a dominant geomorphic process on this portion of sea-exposed coast. This conclusion has been reached by Silvester (1961) and Kempin (1953) for other coastal areas of the Swan Coastal Plain.

Extrapolation of erosional rates derived from the study area (1-2 m/year) into the past suggests at least 1 km of coast has been lost every 1 000 years. This width seems excessive, but even with more conservative estimates, erosion has been the main event in the more recent Holocene at least for this area,

i.e. the Holocene sea has done nothing but erode sediments here since it reached its present level some 3 000-4 000 years ago (Semeniuk in prep.). Stratigraphic evidence (Semeniuk, in prep.) also indicates that the bulk of the peninsula did not form by progradation of coastal sediments with sea level at its present position. It appears therefore that erosion has been a long term continuing event rather than a short-term event of the more recent Holocene.

Aeolian action, which is relatively quite slow, is redistributing sand toward the east in a series of staggered advances. Marine erosion is far more rapid and severe, and it is responsible for marked shore retreat. The beach sediment at present is characteristically stained orange (Figs. 4A, 7B) and would be quite diagnostic wherever it is deposited.

The bulk of this eroded material does not find its way into the onshore dune environment (Fig. 4A) but is transported north by longshore drift. Beaches north of Myalup (some 25 km north of Bunbury) which were white less than a decade ago, are now receiving orange sand. In contrast, beaches south of the study area are still white. The northward movement of sand has been recognised previously by Kempin (1953) working on coastal areas between Cockburn Sound and Scarborough.

The next point of interest concerns the final resting place of the coastal sands mobilised northwards by shoreline processes. Obviously some is trapped in embayments forming a prograding beach/beach ridge sequence as exemplified by Rockingham Plain. Some forms tombolos in the lee of islands and reefs and is instrumental in the development of embayments such as Cockburn Sound and Warnbro Sound. The bulk of it, however, may have moved even further north and may now occur as the massive coastal dune fields north of Yanchep.

The third point of interest relates to beachrock. The concept that shallowly submerged rocky reefs and ridges develop in the wake of a retreating coast is quite novel. This implies that some similar rocky reefs in shallow waters offshore from beaches on the Swan Coastal Plain may not be Tamala Limestone but cemented residuals of eroded coastal sands.

The final point relates to the easterly migratory sand dunes. Although their movement is staggered it may be expected that ultimately the dunes will migrate across the inlet and abut the hinterland. Quindalup dunes will impinge upon Spearwood dunes. This in fact has already occurred in the vicinity of Binningup. Any further migration would result in Quindalup dunes partially overlying Spearwood dunes. More importantly, the entire Leschenault Inlet sequence could be lost by marine erosion. Thus the variability present today from offshore to the hinterland would be reduced to a more simple west to east parallel sequence of beachrock, beach, Quindalup dunes, Spearwood dunes. This latter sequence is commonly found on the Swan Coastal Plain.

Acknowledgments.—This study was undertaken on behalf of the Public Works Department as part of research into management of effluent disposal in coastal dunes. The funding provided by the Public Works Department is gratefully acknowledged. Fruiitful discussion and logistic aid was provided by Mr R. Green and Mr D. Hayworth. Numerous individuals aided in field work and discussion, notably M. Frisina and T. Doust. R. K. Steedman and Associates supplied meteorologic/oceanographic data and provided helpful discussion on the oceanographic aspects of the manuscript. The manuscript was read critically by 1. Le Provost, P. N. Chalmer and S. Stroud.

References

Australian National Tide Tables (1979).—Australian Hydrographic Publication 11, Australian Government Puhlishing Service, Canberra.

Bretscheider, C. L. (1959).—Revisions in wavc forecasting; deep and shallow water. Proc. Sixth Conference on Coastal Engineering. ASCE Council on Wave Research 1958.

Bureau of Meteorology (1975).—Climatic averages, Western Australia. Australian Government Publishing Service, Canberra.

Bridges, E. M. (1970).—World soils. Cambridge University Press.

Bricker, O. P., (Ed.) (1971).—Carbonate Cements. The Johns Hopkins Press.

Gentilli, J. (1972).—Australian Climate Patterns. Nelson.

Gentilli, J. and Fairbridge, R. W. (1951).—Physiographic diagram of Australia. The Geographic Press, Columbia University, New York.

Hodgkin, E. P. and Di Lollo, V. (1957).—The tides of South-Western Australia. *J. Roy. Society of W.A.*, **41**: 42-54.

Jutson, J. T. (1950).—The Physiography (geomorphology) of Western Australia, 3rd Ed. *Geol. Survey of W.A.* Bull. 95.

Kempin, E. T. (1953).—Beach sand movements at Cottesloe, Western Australia. *J. Roy. Soc. W.A.*, **37**: 35-58.

McArthur, W. M. and Bettenay, E. (1960).—The development and distribution of the soils of the Swan Coastal Plain, Western Australia. Soil Publication No. 16 C.S.I.R.O., Melbourne.

Meagher, T. D. (1971).—Ecology of the crab *Portunus pelagicus* (Crustacea: Portunidae) in South-Western Australia, Ph.D. thesis, University of W.A. (unpublished).

Northcote, K. H., Hubble, G. D., Isbell, R. F., Thompson, C. H., and Bettenay, E. (1975).—A description of Australian soils. C.S.I.R.O., Melbourne.

Playford, P. E., Cockbain, A. E. and Low, G. H. (1976).—Geology of the Perth Basin, Western Australia. *Geol. Survey of W.A.*, Bull. 124.

Rochford, D. J. (1951).—Studies in Australian estuarine hydrology. 1. Introductory and comparative features. *Australian J. Marine and Freshwater Res.*, **2**: 1-116.

Seddon, G. (1972).—Sense of Place. University of W.A. Press.

Semeniuk, V. (in prep.)—Quaternary Stratigraphy and Geological History of the Australind—Leschenault Inlet Coastal Area.

Semeniuk, V. and Blackwell, M. (in prep.)—The terrestrial flora of Leschenault Peninsula.

Silvester, R. (1961).—Beach Erosion at Cottesloe, W.A. Civil Engineering Trans. 27-33.

Sverdrup, H. U. and Munk, W. H. (1947).—Wind, sea and swell; theory of relations for forecasting. Publication No. 601. U.S. Navy Hydrographic Office, Washington, D.C.

Journal of the Royal Society of Western Australia, Vol. 64, Part 2, 1981, pp. 53-64.

The geological setting and origin of emerald deposits at Menzies, Western Australia.

by J. D. Garstone

Woodside Petroleum Development Pty. Ltd., 77 St. George's Terrace, Perth, W.A. 6000

Manuscript received 27 November, 1979; accepted 17 February, 1981

Abstract

Emerald has been found associated with a series of north-west trending irregularly shaped pegmatite veins which are concordantly emplaced along schistosity planes within ultramafic rock at Riverina station, near Menzies, Western Australia. The country rock schists have apparently been formed by potassium metasomatism of the ultramafic rock during intrusion of the pegmatite. On average they contain 0.15% Cr_2O_3 and vary mineralogically from predominantly phlogopite schist to rocks that additionally contain hornblende, actinolite, chlorite and talc. Three reaction zones are developed around the pegmatite: (1) hornblende zone, (2) zone of platy phlogopite, and (3) actinolite zone. Beryl is found in the pegmatite, but is more abundant in the surrounding mica schist. Berryllium-bearing solutions have apparently permeated the ultramafic country rock to a maximum distance of 30 cm and extracted small quantities of chromium. Three stages of beryl crystallisation have been recognised. Colourless and pale green beryls formed first, followed by crystallisation of dark green beryl, coloured by chromium; high alkali, chromium-deficient crystals formed last. Emerald, containing 0.15-0.23% Cr_2O_3, probably formed in phlogopite schist during the intermediate stage.

Introduction

Emerald, with diamond, ruby and sapphire is one of the most sought-after and highly valued precious stones. Consequently, the discovery of emerald at Riverina, west of Menzies, Western Australia, could be of economic significance, and has provided part of the incentive for this study.

Emerald is the gem variety of beryl characterised by its rich green colour due mainly to traces of chromium impurity. Anderson (1966) believes that to be classified as emerald, beryl should be coloured by sufficient chromium to show a clear absorption spectrum with the hand spectroscope. It has recently been recognised that vanadium may produce a similar green hue (Taylor 1967). The question of whether emerald-green beryl containing vanadium is classed as emerald arises when appreciable amounts of this element are present.

Emerald finds have been recorded at several localities in Western Australia. The earliest and most productive deposit is at Poona, in the Murchison Division, where emeralds are found in mica schist and pegmatite. Other minor discoveries have been reported from Wodgina, Warda Warra and Melville. Glover (1968) summarises the literature on these deposits and lists sample material held in public institutions in Perth. Emeralds from these sources are apparently associated with pegmatites and schists, as are most of the world's emeralds, with the notable exception of the Columbian gems.

Very little detailed geological research has been carried out on the genesis of such deposits. It is widely accepted that beryllium is introduced by pegmatites, and that chromium is derived from surrounding ultramafic rocks. The emerald deposit at Riverina is here used to examine this traditional model from a geological standpoint. Emerald is treated as part of the sequence of beryl, which is fairly abundant at Riverina. The geology and geochemistry of the deposit have been outlined by a combination of field mapping and laboratory-based studies. Other aspects examined include: geochemistry and mineralogy of the rocks at the emerald deposit, geochemical trends as potential prospecting guides, crystallisation history of the beryl sequence and origin of coloration of beryl.

Menzies is in the North Coolgardie Goldfield, 121°00'E, 29°40'S, at an altitude of 430 m above sea-level, and is connected with Perth by 725 km of sealed roads via Kalgoorlie. The area under review, where emerald and green beryl were discovered in 1974, lies in a greenstone belt some 46 km west of Menzies, on Riverina station (Fig. 1). Low hills and ridges surrounded by alluvial plains define the north-west trending belt. This is a semi-desert region where annual rainfall is variable, but generally low, and vegetation consists mainly of stunted acacias and mixed scrub.

The Menzies area is underlain by Precambrian rocks (see Fig. 1). Kriewaldt (1970) describes the succession as follows:

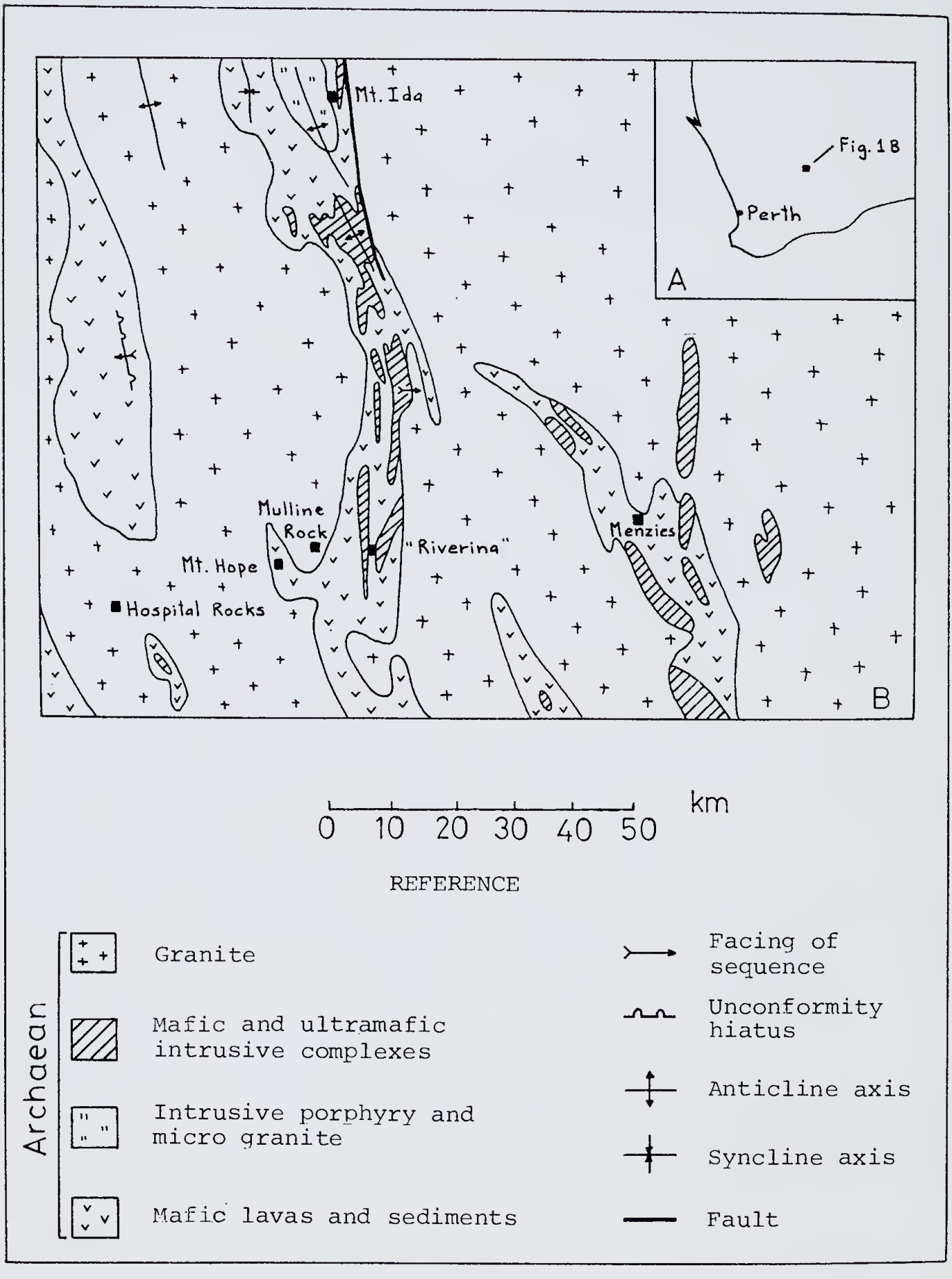

Figure 1.—A. Location map. B. Regional geology of Menzies Sheet SH/51-5 (based on Kriewald 1967).

5. Pegmatite, felsite.
4. Intrusive, granite.
3. Quartz porphyry, ultramafics, and abundant mafic sills which intrude (1) and (2).
2. Talc-chlorite schist, pyritic chert, conglomerate with chert cobbles, basalt, slate, siltstones, grits and acid volcanics.
1. Basalt, quartz-mica schist, slate, greywacke, and banded iron-formation; all intruded by ultramafics.

The layered sedimentary and volcanic rocks are metamorphosed and intruded by a medium-grained biotite granite which is probably about 2 600 m.y. old (Kriewaldt 1970).

Geology of the deposit.

The emerald deposit on Riverina station lies in a greenstone belt that forms part of the Western Australian Archaean Shield. Outcrop is poor and exposure is limited to a sizeable open-cut and several shallow exploration costeans. The geological setting comprises a fairly simple sequence of altered volcanic and ultramafic rocks, intruded by acid veins and dykes (Fig. 2). Beryl and emerald mineralisation are associated with a series of narrow pegmatite veins which intrude the ultramafic rocks. The pegmatite zones will be discussed separately.

Mafic metavolcanic rock

A metamorphosed mafic volcanic unit dominates outcrop in the area and forms low ridges along its contacts with the ultramafics. It is traversed by numerous small randomly-oriented quartz veins. The schistosity of this dark grey, fine-grained unit has a northerly strike. The mafic rock is composed of chlorite, green amphibole and plagioclase, and is clearly metamorphic and of probable volcanic origin. Although usually schistose, microstructures observed in thin-sections of several samples appear to preserve an original texture which has survived amphibolite-facies metamorphism. Typically, small anhedral grains of plagioclase are randomly dispersed throughout the chlorite-amphibole schist; samples showing microstructures contain small, flattened pods of plagioclase enclosed in the matrix schist. These pods may be relict amygdales of an original basalt, or the relict texture of a volcanic agglomerate.

Ultramafic rock

The ultramafic body, approximately 120 m wide, is bounded to the east and west by the mafic metavolcanics already discussed. Relative to the low north-south ridges formed at these contacts, its surface expression is a narrow flat crossed by several small intermittent creeks. Superficial deposits resulting from *in situ* weathering of the ultramafic body mask the underlying rocks. Quartz and acid intrusives crop out but only surface rubble indicates the presence of the ultramafic unit. Relict spinifex texture preserved in a large block of ultramafic rock exposed in the open-cut indicates that it is an ultramafic komatiitic lava flow. A small bed of intercalated ferruginous sediments has been intersected in a shallow costean.

The ultramafic body has been metamorphosed to schist of variable mineralogy. Chlorite schist close to the surface accounts for the dark green appearance of the ultramafic rubble. It probably represents a retrograde phase of metamorphism and results from the hydration and alteration of higher grade ultramafic rock. At the open-cut, where the rocks are exposed to a depth of 7 m below the surface, the ultramafic schist is interfoliated with the mica schist developed at the margins of pegmatite veins. It consists of a crenulated tremolite/actinolite-phlogopite/biotite assemblage. Bladed spinifex texture is preserved by grains of phlogopite cross-cutting a lineated tremolite/actinolite groundmass.

Near-surface material stripped from the site of the open-cut also contains pale-green talcose schist, and chloritic rock traversed by small veins of carbonate and fibrous white asbestos. Talc schist is exposed at depth in the face of the pit and is probably related to the suite of altered rocks bordering the pegmatite. The carbonate and asbestos veins are secondary and restricted to the weathering zone.

Whole-rock analyses of two typical samples of actinolite-phlogopite schist (DUB 1 and 2) show a composition intermediate between basaltic komatiite and peridotitic komatiite. Their chromium content is quite high (0.18-0.31% Cr_2O_3), and the amount of silica they contain places them on the border between basic and ultrabasic rock (See Table 2).

Acid intrusives

A number of acid veins and dykes intrude the volcanic sequence, particularly the ultramafic body, and may be classed as: quartz vein, quartz-feldspar porphyry and granitic vein. These intrusives generally strike east-west; only small quartz veins follow the north-eastward trend of the pegmatite. Field observations and chemical analyses indicate that they are not related to the beryl mineralisation.

The pegmatite

The pegmatite comprises a series of north-east trending veins concordantly emplaced along schistosity planes within the ultramafic body. Some veins are almost wholly composed of feldspar, whereas others contain only blocky quartz or quartz-feldspar intergrowths. They do not resemble the typical pegmatites of granitoid terrains. A striking feature of these veins is the development of phlogopite schist along their margins. Beryl occurs in the pegmatite, but the darker green and emerald varieties, in particular are more abundant in the schist.

The pegmatite is a classic example of what Beus (1962) refers to as a "granitic pegmatite of the crossing-line". Characterised by specific mineralogic-geochemical peculiarities, crossing-line pegmatite fields usually lie in the exo-contact zones of pegmatite-bearing granitic intrusions in metamorphosed mafic and ultramafic rocks. These veins are complex and it is difficult to ascertain whether they are indeed pegmatitic, or more closely related to hydrothermal and pneumatolytic processes.

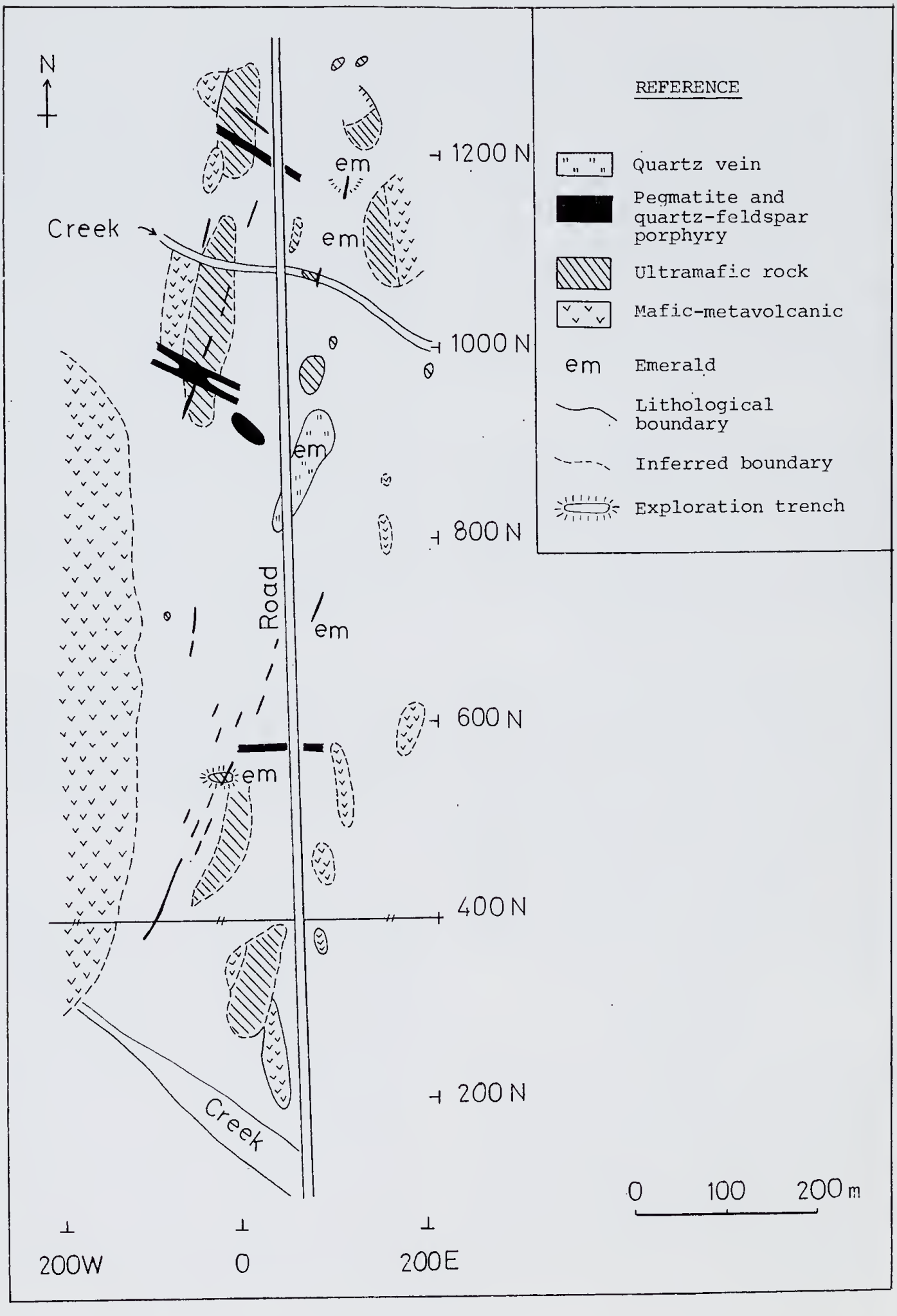
N
Creek
em
em
em
em
em
em
Road
Creek
1200 N
1000 N
800 N
600 N
400 N
200 N
200W
0
200E
0
100
200 m
REFERENCE
Quartz vein
Pegmatite and quartz-feldspar porphyry
Ultramafic rock
Mafic-metavolcanic
em Emerald
Lithological boundary
Inferred boundary
Exploration trench

Structure

The pegmatite veins are generally narrow and very irregularly distributed. Their presence is marked by platy black phlogopite schist. Auger drilling to a depth of 1.2-3.0 m aids geological mapping and is particularly valuable in tracing the mica schist-pegmatite zone. Narrow discontinuous fingers of schist have a general north-east trend; the widest developments are at the site of the open-cut and at the intersection with the road.

The structure of the pegmatite is complex and consists of narrow veins up to 0.5 m wide that unite and diverge. Small discrete lenses of feldspar (1-5 cm in length) in phlogopite schist are normally found less than 10 cm from quartz and quartz-feldspar veins. In places, large feldspar lenses are clustered into 'podiform' veins.

Reaction zones

The intrusion of pegmatite veins has resulted in contact metamorphism and metasomatic alteration of the ultramafic host rocks. Zonal structure is characteristic of veins in which feldspar predominates, but not of podiform feldspar and quartz-rich veins. It is evident that volatiles and chemically active fluids which permeated the country rock are closely related to the feldspathic fraction of the pegmatite. In a contact reaction zone such as this, where a concentration gradient is established, mica and amphibole tend to nucleate more easily than other minerals. Three major reaction zones have been formed:

(1) *Hornblende zone.* Acicular blades, frequently altered to bright green clay, penetrate the phlogopite schist bordering feldspar veins. In some hand specimens these blades account for about 40% of the rock, whereas in others they are sparse. The green clay was identified by X-ray diffraction as saponite—a magnesium member of the montmorillonite group, commonly associated with mineral veins (Deer *et al.* 1966). The green blades of clay are the final alteration product of a green hornblende which probably has an unusual composition. Some crystals are weakly zoned. The hornblende forms euhedral crystals, most of which have undergone varying degrees of alteration. The most common alteration product is chlorite and a mineral identified as possibly stilpnomelane.

Hornblende has thus undergone several stages of alteration. Textural evidence suggests that the order of alteration is probably as follows:

hornblende → stilpnomelane → chlorite → saponite.

Preservation of the bladed morphology of the parent hornblende, even when completely broken down to saponite, indicates hydrothermal alteration, probably from pegmatitic waters recirculating during crystallisation.

(2) *Zone of platy phlogopite.* This is the widest reaction zone and encompasses the hornblende zone. Along podiform feldspar veins and quartz-rich veins the hornblende zone is absent, in which case the platy phlogopite zone is developed at vein margins. Clusters and single crystals of beryl, especially emerald, are found in fine lamellar phlogopite.

Phlogophite schist enclosing feldspar pods is intensely folded and deformed. Veins, about 0.2 m wide, of strongly interlocked phlogopite are less common. They have a recrystallised appearance and generally mark the border between phlogopite schist and large bodies of actinolite-bearing ultramafic schist. Minor yellowish green beryl is present.

(3) *Actinolite zone.* The actinolite zone is irregularly shaped and developed intermittently as separate elongate lenses and bands, ranging from a fraction of a centimetre to several centimetres in width. The rock is almost entirely composed of actinolite and phlogopite and is interfoliated with platy phlogopite schist at the intersection of the two zones.

Although the hornblende and phlogopite zones are intimately related to the pegmatite, the actinolite zone apparently represents remnants of the original ultramafic country rock which have been only moderately altered. The medium-grained actinolite rock is schistose and in places severely deformed by microfolding. Crenulation cleavage is developed in some rocks.

Microfolds are present in thin-sections of specimens UB3* and DUB2. Structures and textures in these thin-sections have important implications regarding the paragenesis of the phlogopite. Phlogopite tends to be concentrated along fold axes. A number of phlogopite grains seem undisturbed by the fold axis, whereas actinolite grains aligned along schistosity planes are fractured. It can be inferred that phlogopite formed during the deformation that is assumed to have been coincident with intrusion of the pegmatite. Hence, the phlogopite metasomatism is almost certainly related to emplacement of the pegmatite. Actinolite schist lies farthest from the pegmatite veins and represents the outer limit to which potassium, necessary for the formation of phlogopite, permeated the ultramafic. In the hornblende and platy phlogopite zones the rocks contain mainly phlogopite. Datta (1966) suggests that potassium may form phlogopite by reaction with the Mg-silicates of an ultramafic rock.

Talc and chlorite schist are also found in the sequence of altered rocks surrounding the pegmatite. Beus (1962) includes chlorite and talc zones as part of the reaction complex characteristic of beryl-bearing veins of crossing-line pegmatites, together with the phlogopite and actinolite zones discussed previously. At Riverina the talc and chlorite rocks are randomly distributed and cannot be assigned to specific zones. They lie farthest from the pegmatite veins, beyond the actinolite zone, and result from alteration and hydration of the ultramafic country rock.

Geochemistry and mineralogy

The face of the open-cut is the largest exposure of the pegmatite (38 m long, 7 m deep) and was chosen as the main site for a geochemical survey. Mica schist is widely developed around massive and podiform feldspar veins and large blocky quartz veins.

* Representative specimens held in the Geology Department Collection, University of Western Australia. (Specimen numbers 85821-85851).

Figue 2.—Surface geology of Lease 30/1243. Grid coordinates are referred to the north-south baseline.

Most of the talc and chlorite schist has been removed during early excavation to expose the mica schist zone. This is the only location where reaction zoning is clearly defined.

In areas such as this, where the rocks are very heterogeneous, sampling is difficult and results tend to reflect the sampling techniques employed. Some of the problems encountered include: (1) sporadic distribution of beryl, both within the pegmatite and mica schist, (2) interfoliation, on a centimetre scale, of mica and actinolite schist, (3) most rocks, even at depth are extensively altered. Feldspar and hornblende have been hydrothermally altered, probably during the late stages of crystallisation of the pegmatite. Any geochemical trends likely to serve as useful prospecting guides must be established for these altered rocks, since fresh material is rare, (4) small-scale zonal structure in which zone boundaries are gradational and (5) limited outcrop of individual pegmatite veins.

Many of the rocks and minerals were collected only centimetres apart to detect possible compositional changes. Twenty-six samples were collected *in situ* from the open-cut and 10 samples were taken from dumps of material stripped from the schist zone (Table 1).

Table 1

List and description of analysed samples

Sample No.	Description of Sample	Analysis†
S5	Phlog. schist along small vein of qtz-feldspar pods.	1
S6	Phlog. schist along small vein 0·7 m above S5.	1
S2	Soft phlog. schist, abundant green blades of clay.	2
S8	Soft phlog. schist. abundant green blades.	1
S3	Phlog. vein sample, strongly interlocked grains.	1
S4	Phlog. schist enclosing blocky qtz vein—no association with feldspar or beryl.	1
S9	Phlog. schist—small green blades, dark green beryl.	1
S10	Phlog. schist 0·2 m below S9, more beryl present.	1
B1	Medium green beryl crystal from S10, close to felspar.	2
F6	Moderately altered cream feldspar.	2
S12	Phlog. schist bordering F6—coarse green blades, some dark green beryl.	1
F1	Yellowish altered feldspar.	2
S13B	Beryl-bearing phlog. schist adjacent to F1	2
S13C	Beryl-bearing phlog.—abundant green blades.	1
S13D	Contorted schist further from F1, adjacent to S13C.	1
F2	Fresh white feldspar from large podiform vein.	2
S14B	Crenulated phlog. schist enclosing pod of F2	2
B4	Pale emerald green beryl crystal from S14B.	2
S14C	Soft ultramafic interfoliated with S14B.	1
F4	Fresh feldspar from beryl-bearing vein.	2
F5	Fresh feldspar from beryl-bearing vein.	2
S19C	Phlog schist—green blades present.	1
S19E	Phlog. schist adjacent to feldspar vein—contains dark green beryl.	2
UB1	Dark grey-green ultramafic—relict spinifex texture.	1
UB2	Fe-stained ultramafic from trench where beryl occurs.	1
UB3	Schistose ultramafic closely interfoliated with phlog. schist.	1
*DS9	Phlog. schist near feldspar vein—green-blades present.	2
*DUB1	Schistose ultramafic 2 cm from sample DS9.	2
*DS10	Phlog. schist.	2
*DUB2	As above.	2
*F7	Cream-white feldspar, beryl present.	2
*B3	Pale blue-green beryl from F7.	2
*B2	Massive aggregate of dark green, opaque beryl crystals in phlog. schist.	2
*DF16	White feldspar—no association with beryl.	2
*DS2	Phlog. schist containing dark green beryl.	2
*F3	Feldspar (microcline) from qtz-feldspar porphyry near open-cut.	2

Bracketed samples are from the one location.
* Denotes specimens collected from dumps at the treatment plant (i.e. not *in situ*).
†1—AAS analysis for Be, Na, Cr only. 2—Whole-rock analysis.

Ultramafic rock and phlogopite schist

Whole-rock analyses were carried out on 9 samples of ultramafic rock and phlogopite schist (Table 2). Partial analyses for Be, Na, and Cr were carried out on a further 15 samples (Table 3).

Visible beryl crystals were removed from samples before crushing to ascertain whether beryllium is held exclusively in these crystals or is disseminated through the country rock. Results show that up to 312 ppm Be is held either in micro-crystals of beryl or substituted into mica. Beryllium was evidently introduced by the pegmatitic fluids and has permeated the country rock to a maximum distance of 30 cm from pegmatite veins. It is closely associated with feldspar; no trace of beryllium was detected in phlogopite schist enclosing a large, blocky quartz vein. The concentration of beryllium diminishes with distance from the pegmatite; the actinolite zone contains typically low values of about 30 ppm Be. There is, however, no correlation between the concentration of disseminated beryllium and the presence of large beryl crystals.

Schist from the actinolite zone has undergone only moderate alteration by fluids emanating from the pegmatite and hence approximates the composition of the original ultramafic country rock. Its magnesium content of 15-17% MgO indicates a composition intermediate between basaltic komatiite and peridotitic komatiite, but its chromium content is high. Potassium and aluminium, introduced by the invading pegmatite, are enriched in the platy phlogopite and hornblende zones. These zones grade into the ultramafic rock, and the igneous parentage of the phlogopite schist is established by its persistently high chromium content (0.15-0.32% Cr_2O_3). Chromium has evidently not been introduced from elsewhere, and it is concluded that the phlogopite schist was formed by metasomatic alteration of the original ultramafic country rock.

To sum up, the actinolite and phlogopite schist show little compositional variation. Beryl is randomly distributed but limited to within 30 cm of feldspathic pegmatite veins. No geochemical indicators of the presence of beryl in schist are apparent.

Feldspar

Feldspar from 6 pegmatite veins was sampled and analysed. Sample F3 was collected from a large quartz-feldspar porphyry vein near the open-cut (Table 4). The chemical composition of pegmatitic feldspar is quite uniform. Relatively high K_2O, H_2O and MgO contents are attributed to the presence of sericite. Sericitisation probably occurred during the main phase of potassium metasomatism that formed phlogpite reaction zones.

Table 2

Whole-rock analyses of ultramafic rock (um.) and phlogopite schist samples

Wt. %	DUB 1 (um.)	DS 9	DUB 2 (um.)	DS 10	S 2	S13B	S14B	S19E	DS2
SiO_2	46.83	42.88	44.81	42.99	43.61	42.45	42.34	42.42	43.36
TiO_2	0.38	0.39	0.29	0.37	0.25	0.37	0.37	0.37	0.38
Al_2O_3	9.57	12.57	11.18	12.93	12.16	12.48	12.34	12.39	12.07
Cr_2O_3	0.18	0.25	0.31	0.24	0.18	0.15	0.18	0.24	0.22
Fe_2O_3	1.77	2.23	3.41	2.20	3.96	2.81	2.81	2.39	1.88
FeO	8.25	7.53	7.46	7.41	5.14	6.81	7.11	7.20	7.54
MnO	0.23	0.13	0.16	0.12	0.07	0.11	0.14	0.19	0.13
MgO	17.24	17.78	15.65	18.29	17.78	19.54	19.18	19.90	18.69
CaO	6.37	1.88	3.87	1.41	0.14	0.74	0.08	0.01	1.79
Na_2O	0.81	0.55	0.86	0.56	0.56	0.39	0.42	0.44	0.43
K_2O	3.33	5.57	4.14	6.77	6.14	7.19	7.84	7.88	6 84
H_2O^+	2.08	3.15	2.61	3.51	3.38	3.16	2.34	2.56	2.18
H_2O^-	1.55	2.32	2.39	1.51	3.52	1.61	2.41	2.33	2.30
P_2O_5	0.02	0.06	0.02	0.11	nil	0.09	0.06	0.02	0.01
Be (ppm)	37.0	87.5	31.2	100.0	nil	62.5	12.5	75.0	312.5
Total*	98.61	97.29	97.16	98.42	96.89	97.90	97.62	98.34	97.82

*Consistently low totals are probably due to the presence of small amounts of copper and nickel which were not analysed for.

Microcline is the common feldspar in east-west trending quartz-feldspar porphyry veins near the open-cut. It contains no trace of beryllium or Li_2O. This accords with the view that the porphyry is not related to the beryl mineralisation.

Beryl

The properties of Riverina emerald are as follows (MacKay pers. comm. 1977):

Optical properties

R.I.: 1.573-1.581
Birefringence: 0.008
Optical character: negative
Dichroism: blue-green and yellow-green
U.V. light: inert (due to high ferric oxide content)
Chelsea Filter: brown to pink
Spectroscope: typical for Cr coloured gems; fine absorption lines in red; broad absorption in yellow-green; broad absorption in violet.

Table 3

Be, Na and Cr analyses of ultramafic (um.) and phlogopite schist samples

Sample No.	Be (ppm)	Wt. % Cr_2O_3	Wt. % Na_2O
S3	nil	0.32	0.40
S4	nil	0.25	0.30
S5	nil	0.08	0.41
S6	nil	0.05	0.31
S8	25.0	0.20	0.50
S9	25.0	0.19	0.36
S10	100.0	0.21	0.34
S12	62.5	0·25	0.50
S13C	37.5	0.28	0.83
S13D	25.0	0.24	0.30
S14C	12.5	0.18	0.44
S19C	31.2	0.27	0.51
UB1 (um.)	37.5	0.32	0.73
UB2 (um.)	37.5	0.10	0.31
UB3 (um.)	37.5	0.30	0.52

Table 4

Feldspar analyses. All samples, except F3, contain traces of beryllium

Wt. %	F1 (vein 1)	F2 (vein 2)	F3 Qtz-Feldspar Porphyry	F4 (vein 3)	F5 (vein 3)	F6 (vein 4)	F7 (vein 5)	DF16 (vein 6)
SiO_2	62.26	59.34	65.24	57.98	60.31	57.57	59.54	58.90
TiO_2	nil	nil	nil	nil	nil	nil	nil	nil
Al_2O_3	22.33	25.40	19.21	24.82	24.18	24.61	24.48	25.31
Cr_2O_3	nil	nil	nil	nil	nil	nil	nil	nil
Fe_2O_3	1.27	0.28	0.16	0.84	0.61	0.82	0.31	0.23
FeO	0.09	0.11	0.02	0.17	0.09	0.14	0.08	0.22
MnO	0.01	0.01	nil	0.01	0.01	0.01	0.01	0.01
MgO	0.82	0.41	0.06	0.47	0.80	0.89	0.40	0.75
CaO	0.60	1.16	0.04	1.25	0.91	1.08	0.83	1.11
Na_2O	5.12	7.08	1.95	7.08	6.47	6.94	7.14	8.09
K_2O	3.28	4.01	12.60	3.55	3.27	3.36	3.67	3.35
Li_2O	0.02	0.02	nil	0.02	0.03	0.02	0.02	0.03
Cs_2O	0.14	0.14	0.14	0.16	0.15	0.14	0.17	0.15
H_2O^+	2.38	1.76	0.09	1.98	2.59	2.53	2.24	1.90
H_2O^-	1.63	0.61	0.01	1.08	1.12	1.47	1.03	0.39
P_2O_5	0.01	nil	0·02	nil	0·01	0.01	0.01	nil
Total	99.96	100.33	99.54	99.41	100.55	99.59	99.93	100.44

Physical properties

Specific gravity: 2.71-2.75

Inclusions

Healed fractures, many perpendicular to optic axis
Biotite/phlogopite feathers and flakes
Two-phase inclusions (liquid and gas)
Tremolite (?) rods parallel to optic axis.

Analysis

0.23% Cr_2O_3, determined by Atomic Absorption Spectroscopy (Israel).

Geologic association of beryl. Beryl is found in the pegmatite but is often more abundant in the surrounding mica schist. Its colour is a rough index of composition and varies from green and yellow-green to blue-green. Samoilovich *et al.* (1971) propose that the whole range of beryl colourings, from yellow to blue, may be due to the relative concentrations of Fe^{3+} and Fe^{2+} impurity ions in different coordinations. The classification of emerald, without relying on chemical analysis, is rather subjective. In the field only the rich green hue of the emerald variety distinguishes it from common beryl. Unless specifically described as the emerald-green variety, green or dark green beryl referred to in the following sections is assumed to be coloured by iron impurities.

In the pegmatite most of the beryl crystallises as milky blue-green euhedra in albite. Fewer crystals are found in quartz, but they generally have greater transparency. Beryl embedded in feldspar and quartz is normally highly fractured and healed by quartz.

The distinctive coloration of beryl at Riverina distinguishes it from the Poona deposit where only white and colourless beryl are found in the pegmatite (Graindorge 1974). This implies that either iron, which is responsible for the coloration of common beryl, was relatively enriched in the fluids which formed the pegmatite at Riverina, or that these fluids experienced greater interaction with the surrounding ultramafic rock.

Table 5

Beryl analyses

Wt. %	B1	B2	B3	B4
SiO_2	64.22	64.55	65.06	64.23
TiO_2	nil	nil	nil	nil
Al_2O_3	16.53	16.99	16.96	16.47
Cr_2O_3	0.08	0.04	0.06	0.15
V_2O_3	0.02	0.02	0.02	0.02
Fe_2O_3, FeO	0.93	0.84	0.78	0.94
BeO	12.72	12.95	12.99	13.07
MnO	nil	nil	nil	nil
MgO	1.29	0.89	0.86	1.04
CaO	nil	nil	0.03	nil
Na_2O	1.13	1.28	0.60	1.44
K_2O	0.11	0.04	0.08	0.07
Li_2O	0.04	0.04	0.04	0.05
Cs_2O	0.10	0.13	0.02	0.14
H_2O^+	2.40	1.96	1.95	2.01
H_2O^-	0.03	0.01	0.07	0.02
P_2O_5	0.01	nil	nil	nil
Total	99.61	99.74	99.52	99.65

Sample colours, according to the Pantone Matching System, are B1—green (Pantone 346), B2—yellow-green (Pantone 351), B3—blue-green (Pantone 338), B4—emerald green (Pantone 334).

Chemical analysis of blue-green beryl (specimen B3) separated from feldspar reveals the presence of 0.06% Cr_2O_3, 0.02% V_2O_3 and 0.86% MgO (Table 5). These elements are normally removed from a magma during early crystallisation and separation of chromite and ferromagnesium minerals. Their presence in the pegmatite phase suggests they have been incorporated from the ultramafic country rock during crystallisation of the pegmatite.

Beryl in the mica schist is restricted to the hornblende and platy phlogopite zones and displays a wide range of colour and crystal form. Common green and yellow-green beryl is most abundant. Rarer emerald is almost exclusively found in platy phlogopite schist, although several pale crystals have been found intergrown with quartz and feldspar at the vein-schist contact. Three crystals of goshenite (colourless beryl) have also been found.

Hexagonal prisms up to 2 cm in length are common and are usually aligned along schistosity planes. In many places porphyroblastic textures are present, indicating growth of the crystals in a solid state. Radial and bent crystals are found rarely. Goshenite has a tabular habit and prism faces are striated parallel to the c-axis. Emerald occurs generally as single, prismatic crystals embedded in the folio of phlogopite schist.

No pattern is evident in the distribution of coloured beryl. This poses the problem of why some beryl crystals contain chromium impurities, whereas others contain mainly iron. One solution would be the partitioning of elements such as chromium, iron, and vanadium between the beryl and schist adjacent to it. Emerald would be expected to crystallise in phlogopite schist with high chromium content; common green and colourless beryl in schist with low chromium content. However, it is common to find beryl crystals, ranging from yellow-green to dark green, closely associated in a small area of phlogopite schist. Less commonly, emerald crystals are found only several millimetres from drab yellow-green beryl. Such small-scale compositional changes in the schist are unlikely; hence partitioning of elements between beryl and the adjacent schist cannot be responsible for the colour difference. Rather, it seems that a time factor is involved. Incorporation of elements, such as chromium, into beryllium-bearing solutions apparently depends on the length of time that they remain in contact with the ultramafic host rock. This is discussed further in the following sections.

Chemical analysis. Beryl from the pegmatite and mica schist was sampled and analysed. Blue-green beryl (B3) was separated from feldspar. Other beryl samples extracted from phlogopite schist vary from dark green (B1 and B2) to pale emerald green (B4). In general, beryl crystals become progressively darker in colour with increasing distance from the pegmatite.

Chromium in the range 0.14-0.50% Cr_2O_3 produces the unique emerald colour. Sample B4 contains sufficient chromium to be classified as emerald, as defined by Anderson (1966), but the other beryl samples contain only 0.04-0.08% Cr_2O_3. No trace of chromium was detected in feldspar from which sample B3 was separated, yet this beryl contains

0.06% Cr_2O_3. This presumably came from the only source of chromium in the area—ultramafic and phlogopite schist. Vanadium is also present, but in amounts too small to influence coloration.

Beryl from the schist has a uniform chemical composition. Pegmatitic beryl differs in that it has low Na_2O and Cs_2O and is the only beryl that contains calcium.

Sodium in the pegmatite is held almost exclusively in albite. The associated beryl contains only 0.60% Na_2O. The concentration of sodium dispersed through the phlogopite schist increases with distance from the pegmatite. Beryl in schist also reflects this trend and its sodium content increases to a maximum of 1.28% Na_2O, indicating progressive alkali enrichment of the fluids which diffused into the country rock. This has important implications for the genesis of beryl.

In normal pegmatites the multigeneration sequences of beryl, crystallising inwards from the vein margins to the cores and metasomatic units, are known to increase in alkali content (Heinrich 1953). There is no simple analogy between the crystallisation trends of crossing-line pegmatites and these more common types found in granitic terrains. The latter are usually zoned and crystallise from the margin to the core. Crossing-line pegmatites, however, occur as narrow unzoned veins. Alkali enrichment of beryl crystals in mica schist at Riverina suggests that they represent the final stage of beryl crystallisation. It is argued therefore that beryl in the schist formed subsequent to crystallisation of the pegmatite veins. Reaction with the ultramafic would be promoted by prolonged circulation of beryllium-bearing fluids and would account for the dark green coloration of beryl in phlogopite schist.

Thin-section study. Beryl in sericitised feldspar forms euhedral crystals, weakly zoned with few inclusions. No alteration is apparent. Crystal forms of beryl in mica schist are more varied. Small clusters and single crystals form well-developed, hexagonal prisms, but beryl also grows profusely as anhedral aggregates partly intergrown with phlogopite. Most of the individual beryl crystals are zoned. Zoning in hexagonal cross-sections is distinguished by marked variations in refractive index. Cêrny and Turnock (1975) have shown that R.I. becomes higher with increasing alkali content. In keeping with the overall alkali enrichment during pegmatite crystallisation, the outer parts of the crystals almost invariably show R.I. and alkali contents higher than those of the cores.

Beryl and hornblende coexist in the hornblende zone. No reaction is observed at grain contacts, indicating chemical equilibrium between the minerals. They have crystallised almost simultaneously, and where the beryl and hornblende compete for the same space, neither asserts a regular crystal form.

Since most of the minerals of rocks associated with the pegmatite were formed almost simultaneously, these externally paragenetic minerals are encountered again as inclusions in beryl. Phlogopite is by far the most frequent mineral inclusion, often extending from the phlogopite schist into the beryl, partly irregularly and partly along cracks parallel to the basal plane. Also, phlogopite laminae are strewn singly throughout the crystal or filed into parallel or irregular rows. Phlogopite is not everywhere well-preserved and some is iron-stained or partially resorbed. Most beryl crystals are studded with dusty opaque grains that are normally dispersed throughout the entire crystal but are also concentrated in bands roughly parallel to the basal plane. Actinolite rods, aligned parallel to the c-axis, are less common; tubes parallel to the c-axis are found rarely.

Syngenetic inclusions, formed during beryl crystallisation, are mainly two-phase inclusions (liquid with gas bubble); no three-phase inclusions are present. The only post-crystallisation inclusion is secondary quartz which heals fractures.

Electron microprobe analysis. Basal sections of two beryl crystals were analysed by electron microprobe to determine whether there is zoning with respect to chromium and to ascertain if there is a correlation between chromium content and colour of beryl. Chromium K values were measured at an average of ten points in each crystal. A theoretical calibration factor to convert K values to weight per cent Cr_2O_3 was calculated by counting the chromite standard and assuming that the beryl had the ideal composition $Be_3Al_2Si_6O_{18}$.

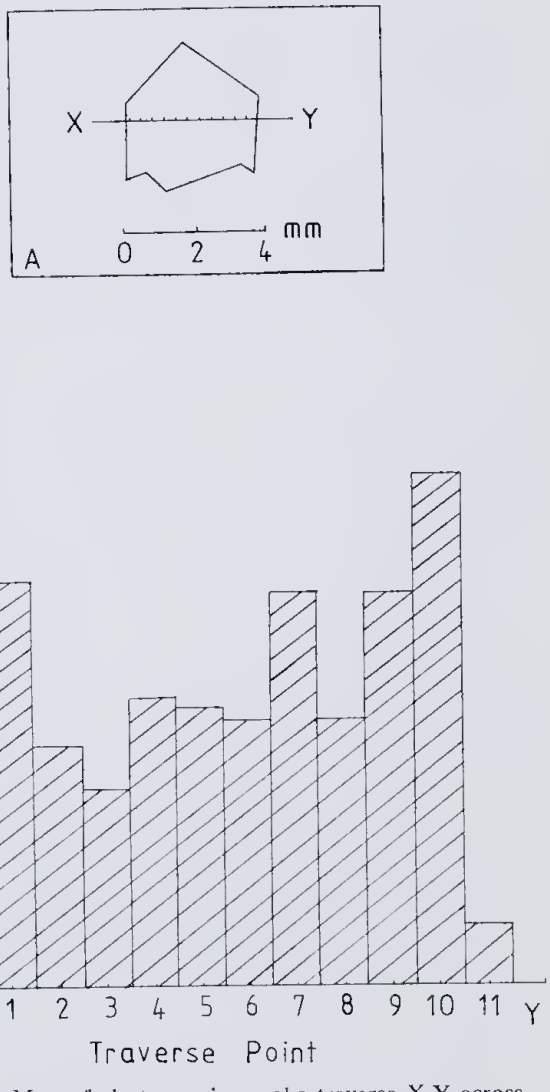

Figure 3.—A. Map of electron microprobe traverse X-Y across the basal section of a blue-green beryl crystal. A complete chemical analysis of this beryl (sample B3) is given in Table 5. B. Variation in weight per cent of Cr_2O_3 along traverse X-Y.

The chomium content of a single blue-green beryl crystal from feldspar (sample B3) varies from 0.05-0.42% Cr_2O_3 (Fig. 3). The variation is irregular, but the outer part of the crystal generally has the highest chromium concentration. A narrow rim of colourless beryl contains only 0.05% Cr_2O_3 (traverse point 11)—insufficient to produce green coloration. This inhomogeneity of composition, even within a single crystal, indicates that bulk chemical analysis only yields an average composition. A complete chemical analysis of another beryl crystal from sample B3 is given in Table 5. Even when taking averaging into account, it contains almost 0.2% less Cr_2O_3 than the crystal analysed by electron microprobe. Hence, chromium content varies not only within single crystals, but also significantly among crystals found only centimetres apart in the same mineralogical environment.

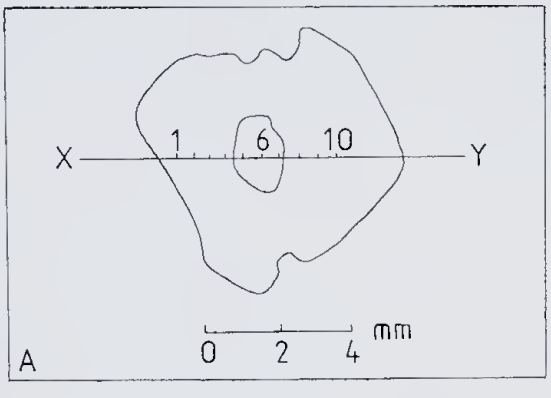

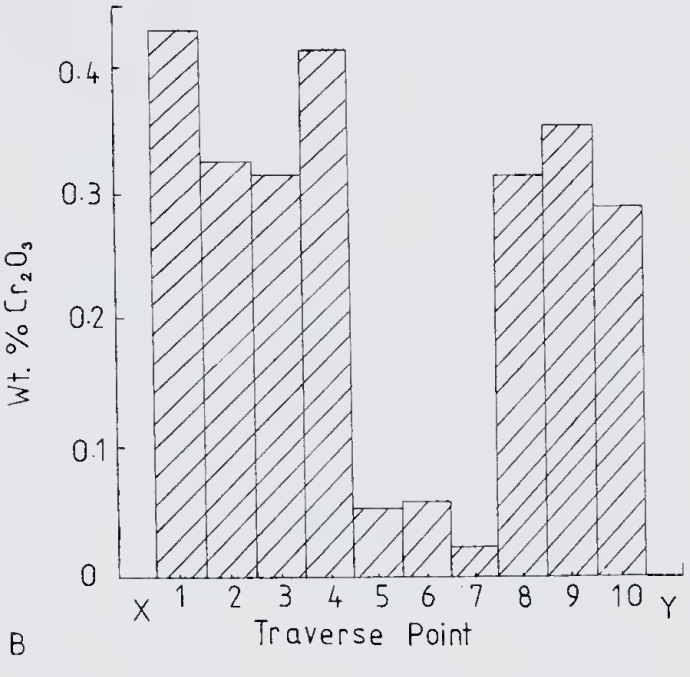

Figure 4.—A. Map of electron microprobe traverse X-Y across the basal section of an emerald-green beryl crystal. Traverse points 1-4 and 8-10 are in the dark green areas and points 5-7 are within the colourless core. B. Variation in weight per cent of Cr_2O_3 along traverse X-Y.

Emerald also has variable chromium content. A correlation between colour and chromium content is clearly established from the results of the analysis of a dark green crystal with colourless core (Fig. 4). The green areas contain a persistently high chromium content of 0.32-0.43% Cr_2O_3, whereas the colourless core contains only 0.03-0.06% Cr_2O_2. Enrichment of chromium in the late growth stages of single crystals of green beryl is characteristic of the Riverina deposit and is an important indicator of their genesis.

Beryl, like many minerals, displays growth anisotropy and grows preferentially in the direction of the c-axis. Its crystals are dominantly bounded by the slowest-growing faces. Colour zoning (and hence partitioning of chromium) is common and may run parallel to prism faces or to the basal plane. Short-term variations in the amount of chromium incorporated into the crystal lattice are recorded by colour changes along the length of the prism. However, zoning in the slowest growing part of the crystal, parallel to the basal plane, implies that fluctuations in the amount of chromium available have been operative over a relatively long time interval.

Gübelin (1956) records the presence of colourless beryl with green cores at Habachtal, Austria, and has assumed therefore that Cr_2O_3 was exhausted during the early phase of beryl crystallisation which resulted in emerald. An earlier phase of colourless beryl crystallisation is, however, evident at Riverina. Within single crystals the Cr_2O_3 content progressively increases outwards from the core. Discrete crystals of high alkali colourless or pale beryl (e.g. goshenite) form last.

In summary, beryl crystallises early as colourless or pale crystals and later as green crystals (including emerald) as chromium is released from the country rock and is incorporated into the mineral lattice. Beryl continues to crystallise when chromium is depleted or exhausted.

Discussion

Literature review

Emerald occurs in two distinct geological environments: (1) biotite and ultramafic schist zones associated with pegmatites and (2) low-temperature veins in sediments. Although schist deposits have been regarded as the "classical" occurrence, most of the world's finest emeralds have come from Columbia, where they are found in veins in sediments. A comprehensive report on the localities and characteristics of the world's known emerald deposits is given by Webster (1975).

Schist deposits. All occurrences of this type include ultramafic rocks or their metamorphic derivatives, which show evidence of pegmatitic activity (Hickman 1972). Situated in igneous-metamorphic terrains, emerald usually occurs in different assemblages of serpentine-biotite-chlorite-tremolite-talc rocks. Emerald has been found in these schistose host rocks in India, Transvaal, Brazil, Urals, Rhodesia, Zambia, the Habachtal (Austria) and a few other less-important localities.

Tourmaline, apatite and minor fluorite often accompany emerald mineralisation. Bank (1974), Muktinah and Banerjee (1969), and others cite the co-existence of these minerals with emerald as

evidence for the migration of volatile-rich pegmatitic fluids into the adjacent country rocks. The colour produced by chromium distinguishes emerald from common beryl and, consequently, interest has been focused on the source of this element. The dependence of the intensity of the green colour upon the quantity of chromium present has been established by Herman and Wussow (1935). Many authors have been content to assume that this chromium is derived from the ultramafic rocks associated with the emerald deposits. Datta (1966), in the study of the Rajgarh Area of India, appears to be the only author who has verified that the ultramafic recrystallised mica schist have a persistently high chromium content (0.11% Cr), compared with low values (0.02% Cr) for the pegmatite.

In summary, it is widely accepted that emerald results, at least in part, from the presence of chrome-bearing rocks of ultramafic association during pegmatite intrusion. This model has been applied to the West Australian emerald deposits at Poona and Menzies by Graindorge (1974) and Whitfield (1975) respectively.

Vein deposits. The major sources of Columbian emerald are the Chivor, Muzo, and Cosquez mines. Johnson (1961) reports that at Chivor emerald is commonly found in 'strings' and 'pockets' in fissure cracks through thick beds of shale. Albite and pyrite are the principal gangue minerals. The geology of the Muzo-Cosquez area is fundamentally similar to Chivor. Here, the emerald-bearing veins, containing calcite, quartz, dolomite and pyrite, run through country rocks of black carbonaceous limestone and shale.

These deposits are unique and the source of emerald mineralisation remains a point of contention. The assumption of hidden igneous rocks at depth seems unsatisfactory as deep erosion has failed to expose them. Feininger (1970) supports an earlier theory that envisages low-temperature formation of emerald by lateral secretion from circulating mineralising waters.

Riverina deposit

Unlike most emerald deposits of this type, the mineralogy of the Riverina deposit is relatively simple. The beryl deposit is not complicated by the presence of other minerals (such as tourmaline, apatite and fluorite) and provides an ideal model to study the paragenesis of beryl. Emerald cannot be studied in isolation because it forms only a small part of the multi-generation sequence of beryl.

Beryllium has been introduced in association with a series of narrow, irregularly shaped pegmatite veins which intrude a large ultramafic body. Phlogopite schist borders the pegmatite veins and grades into actinolite-chlorite-talc schist which comprises the ultramafic country rock. The igneous parentage of this group of schistose rocks is established on the basis of field relations, and their high chromium content (0.15-0.32% Cr_2O_3). Beryl is the only beryllium-bearing mineral formed and is found embedded in the quartz-albite pegmatite and disseminated in the phlogopite schist.

The mineral assemblages of altered rocks in the vicinity of the pegmatite have been formed by metasomatic processes. The country rock consists of actinolite/tremolite, chlorite, talc and chromium. The formation of phlogopite, hornblende and beryl required the introduction of potassium and beryllium. The well-developed fissility and schistosity of these rocks has favoured rich concentrations of volatiles, and phlogopite schist is apparently developed as a result of potassium metasomatism consequent on the emplacement of the pegmatite.

The multigeneration beryl sequence has a complex crystallisation history. Beryllium-bearing fluids have permeated the country rocks to a maximum distance of 30 cm from the pegmatite. Dark green beryl from phlogopite schist has higher alkali content than blue-green beryl from the pegmatite. Fluids are known to increase progressively in alkali content during the pegmatitic crystallisation process, which implies that beryl in the schist formed after crystallisation of the pegmatite veins. Prolonged circulation of beryllium-bearing solutions has apparently promoted reaction with the chrome-bearing ultramafic country rock.

Chromium is present in dark green beryl from the schist, but the results of chemical analysis of a sample of pegmatitic beryl show that it also contains chromium, though in much lower concentration; 0.06% Cr_2O_3 as compared to 0.15% Cr_2O_3 in pale emerald green beryl. Feldspar intergrown with this beryl contains no trace of chromium. It is apparent that beryllium-bearing solutions extract chromium from the ultramafic rocks and crystallise as emerald and dark green beryl. Chromium is not taken up by the other pegmatitic fluids that form the quartz-feldspar pegmatite.

Chromium content varies among crystals and within single, zoned crystals. Colourless and pale green beryl form first, followed by crystallisation of dark green beryl, coloured by chromium, in phlogopite schist. High alkali, chromium-deficient crystals form in the final stage of beryl crystallisation. This shows that chromium is incorporated into beryl during the intermediate stage, some time after intrusion of the pegmatite. The specific source of chromium in the ultramafic country rock has not been determined. Chromite is an extremely refractory mineral and hence an unlikely source. It seems that small amounts of chromium, substituted into mica and other silicates, were released from the ultramafic country rock during its alteration to phlogopite schist.

In summary, the results of this study support the traditional model of formation of emerald. Beryllium and potassium rich solutions from pegmatite veins have penetrated along structurally weak planes in the enclosing ultramafic schist. Potassium reacts with Mg-silicates in the ultramafic rock and forms phlogopite schist; beryllium-bearing solutions extract chromium and crystallise as emerald. Hydrothermal alteration of feldspar and hornblende is effected by the circulation of chemically active fluids during the late stage of crystallisation of the pegmatite. Emerald owes its formation to the complex interaction of pegmatitic, hydrothermal and pneumatolytic processes.

Acknowledgements.—I thank Dr. J. J. E. Glover and Professor P G. Harris for supervising the project; Mr. N. J. MacKay and Mr. P. E. Goodeve for making the project available and providing accommodation during field work; R. F. Lee and W. H. Smeed for providing technical advice and assistance.

References

Anderson, B. W. (1966).—Chromium as a criterion for emerald. *J. Gemmology,* **10**: 41-45.

Bank, H. (1974).—The emerald occurrence of Miku, Zambia. *J. Gemmology,* **14**: 8-15.

Beus, A. A. (1962).—*Beryllium.* Freeman and Company, San Francisco and London.

Cêrny, P. and Turnock, A. C. (1975).—Beryl from the granitic pegmatites at Greer Lake, Southeastern Manitoba. *Can. Mineralogist,* **13**: 55-61.

Datta, A. K. (1966).—Geological milieu of emeralds in the Rajgarh area, Ajmer district, Rajasthan. *Bull. Geol. Soc. India,* **3**: 29-33.

Deer, W. A., Howie, R. A. and Zussman, J. (1966).—*An introdnction to the Rock Forming Minerals.* Longmans, London.

Feininger, T. (1970).—Emerald mining in Columbia: history and geology. *Min. Record,* **1**: 142-149.

Glover, J. E. (1968).—Western Australian emeralds. *Aust. Gemm.,* **10**: 15-17.

Graindorge, J. M. (1974).—A gemmological study of emerald from Poona, Western Australia. *Anst. Gemm.,* **12**: 75-80

Gübelin, E. J. (1956).—The emerald from Habachtal. *Gems and Gemmology,* **8**: 295-309.

Heinrich, E. W. (1953).—Chemical differentiation of multigeneration pegmatite minerals. *Am. Miner.,* **38**: 43.

Herman, F. and Wussow, D. (1935).—The emerald deposits of the world. *Mining Mag.,* **53**: 20-25.

Hickman, A. C. J. (1972)—The Miku emerald deposit. *Ec. Report No.* 27, *Rep. of Zambia, Geol. Snrv. Dept.*

Johnson, P. W. (1961).—The Chivor emerald mine. *J. Gemmology,* **8**: 126-152.

Kriewaldt, M. (1970)—Menzies, Western Australia, Sheet SH/51-5. Geol. Surv. W.A. *1:250 000 Geol. Series Explanatory Notes.*

Muktinah, N. C. and Banerjee, S. N. (1969).—Emerald mineralisation in Rajgarh-Chat-Bithur area, Ajmer district, Rajasthan. *Indian Sci. Congr. Ass., 56th Sess, Proc, Part 3:* 237.

Samoilovich, M. I., Tsinober, L. I. and Duninbarkovski, R. L. (1971) Nature of the colouring in iron-containing beryl. *Sov. Phys.—Crystallography,* **16**: 147-150.

Taylor, A. M. (1967)—Synthetic vanadium emerald *J. Gemmology,* **10**: 211-217.

Webster, R. (1975).—*Gems.* Newnes-Butterworths, London.

Whitfield, G B. (1975). Emerald occurrence near Menzies, Western Australia *Aust. Gemm.,* **12**: 150-152.

Journal of the Royal Society of Western Australia, Vol. 64, Part 2, 1981, pp. 65-68.

Micrognathus spinirostris, a new Indo-Pacific pipefish (Syngnathidae)

by C. E. Dawson and G. R. Allen

Gulf Coast Research Laboratory Museum, Ocean Springs, Mississippi 39564
Department of Fishes, Western Australian Museum, Perth, W.A. 6000

Manuscript received 27 November 1979; accepted 19 February, 1980

Abstract

Micrognathus spinirostris n. sp., characterized by the presence of lateral snout spines, spines on postorbital and posterior supraorbital, branching dermal flaps, notched superior ridge margins and 14 trunk rings, is illustrated and described from Western Australia, Sri Lanka and the Samoa Is. Features of ontogenetic development are described and the species is compared to its most closely related Indo-Pacific congeners (*M. nitidus, M. dunckeri, M. mataafae, M. brocki*).

Introduction

Herald (1953) and Herald and Randall (1972) proposed three subgenera (*Anarchopterus* Hubbs, *Micrognthus* Duncker, *Minyichthys* Herald and Randall) for the accommodation of nominal species of the syngnathine (tail-pouch) genus *Micrognathus* Duncker 1912. However, *Micrognathus* has never been diagnosed or differentiated adequately from other genera with the same configuration of principal body ridges (e.g. *Halicampus* Kaup, etc.) and subgeneric treatment is premature. Absence of an anal fin is here considered sufficient basis for restoring generic rank to *Anorchopterus* which now includes two western Atlantic species, *A. criniger* (Bean and Dresel) and *A. tectus* (Dawson). Relationships of other nominal species of *Micrognathus* remain uncertain, pending completion of a review of these forms presently in preparation. Among recently examined Indo-Pacific pipefishes, there are several undescribed species referrable to *Micrognathus* sensu Herald (1953). Most of these are represented by juveniles, damaged or poorly preserved specimens, but adequate material has been accumulated to permit description of one of the more distinctive forms.

Examined material is deposited in collections of the Academy of Natural Sciences of Philadelphia (ANSP), Bernice P. Bishop Museum (BPBM), Gulf Coast Research Laboratory Museum (GCRL), United States National Museum of Natural History, Smithsonian Institution (USNM) and the Western Australian Museum (WAM). Measurements are in millimetres (mm), proportional values are referred to standard length (SL) or head length (HL), depths are in metres (m); for other methods see Dawson (1977).

Micrognathus spinirostris n. sp.

Figs. 1-3

Material examined: Five specimens, 23.8-103.0 mm SL, including holotype and one paratype.

Holotype: WAM P.26479-001 (103.0 mm SL, male), Western Australia, North West Cape, off Tantabiddi Creek (21°55'S, 113°15'E), outer reef, 10 m, 19 May 1976, G. R. Allen coll.

Paratype: GCRL 16801 (69.0 mm SL, immature or female), locality as for holotype, 8-10 m, 27 June 1975, G. R. Allen coll.

Other material: Sri Lanka (Ceylon): ANSP 142643 (1, 62.5); USNM 220882 (1, 23.8). Samoa Is., Tutuila I.: BPBM 18718 (1, +69.0, damage).

Diagnosis: Trunk rings 14; ridges distinctly notched or indented between rings; head and body with branching dermal flaps; subadults and adults with 2-3 spine-like projections on median dorsal snout ridge, 3 lateral spines on snout, spines on postorbital and posterior supraorbital, and a distal subterminal notch in superior ridges of rings; without alternating narrow bands of pale and dark brown.

Description: Rings 14 + 33-35; subdorsal rings 1.25-0.75 + 3.25-3.75 = 4.25-4.75; dorsal-fin rays 19-20; pectoral-fin rays 13 (in 3 counts)-14 (in 6); anal-fin rays 3; caudal-fin rays 10. Measurements (mm) of holotype and paratype (in parentheses) follow: SL 103.0 (69.0), HL 9.1 (6.7), snout length 2.9 (1.9), snout depth 1.3 (1.0), length of dorsal-fin base 8.2 (5.7), anal ring depth 4.3 (2.4), trunk depth 4.1 (2.3), pectoral-fin length 2.2 (1.4), length of pectoral-fin base 1.7 (1.1).

Superior trunk ridge arched slightly dorsad in subdorsal region (Fig. 1), discontinuous with superior tail ridge near rear of dorsal fin; lateral tail ridge ends without deflection on anal ring; lateral trunk ridge confluent with inferior tail ridge near anal ring; inferior trunk ridge ends at anal ring; venter of trunk slightly V-shaped, without longitudinal keel; dorsal-fin base not distinctly elevated.

Head length about 10 in SL; snout short (3.1-3.5 in HL), its depth 1.9-2.2 in snout length; median dorsal snout ridge (Figs. 1-2) with 2-3 flat spine-like projections, the posteriormost terminates distally in

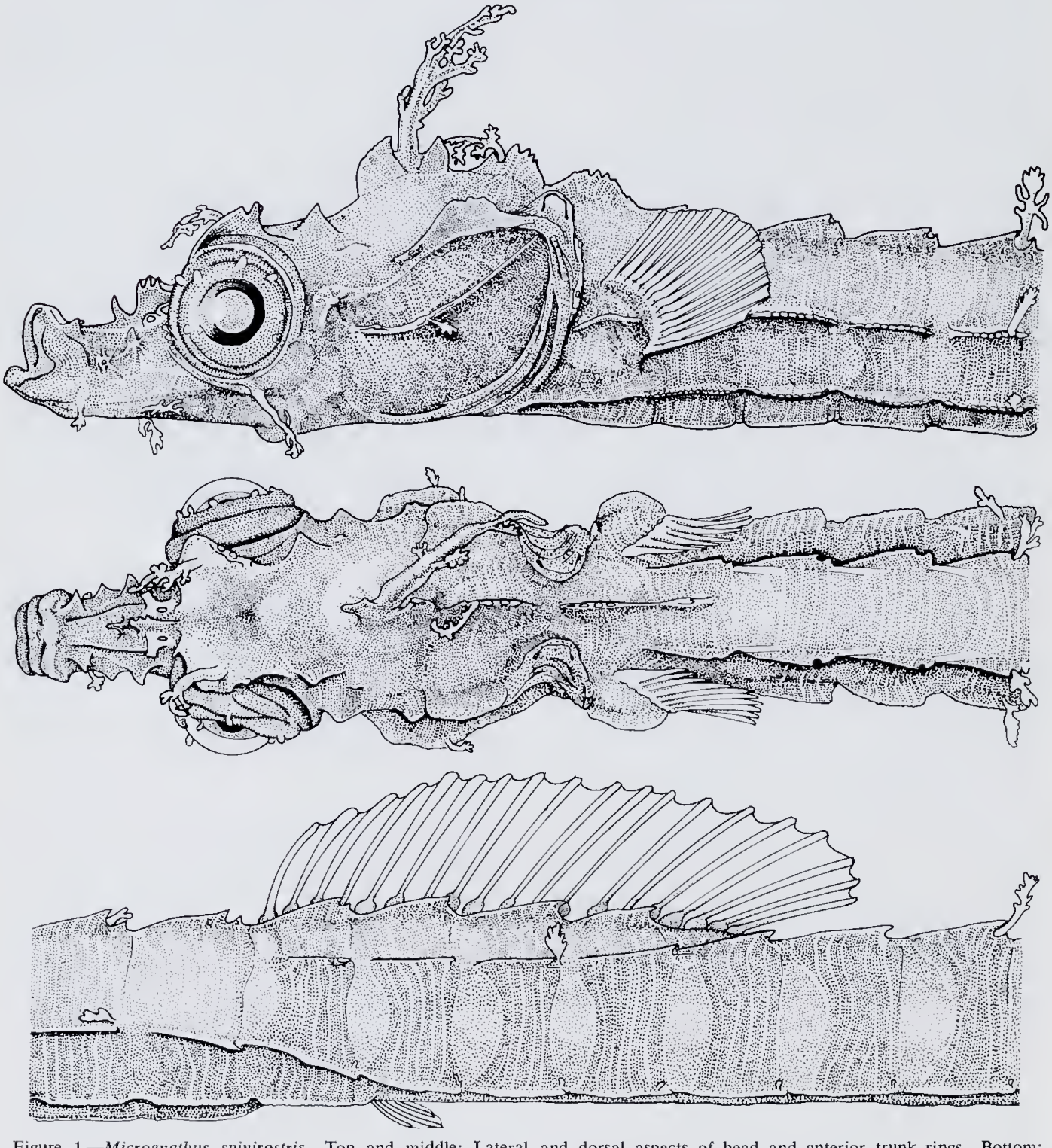

Figure 1.—*Micrognathus spinirostris*. Top and middle: Lateral and dorsal aspects of head and anterior trunk rings. Bottom: Section of body illustrating ridges, dorsal and anal fins. From GCRL 16801 (69 mm SL, paratype).

2-3 points, whereas the remainder have entire margins; side of snout with three distinct, flat to conical, spines; one dorsolateral on anterior third of snout, one midlateral near middle of snout and another just above midlateral axis near vertical from penultimate projection on median dorsal ridge. Rim of orbit with 1-2 minute spines directed anterolaterad near level of nares, one slightly above level of dorsal margin of snout and another on posteroventral portion of rim; inferior portion of orbit flared outward from side of head, its edge irregularly emarginate, and terminates posteriad in a flat spine-like projection; supraorbital ridges broad, flared dorsolaterad from the depressed interorbital, the margins entire in front but with 3-4 spine-like points posteriad; posterior supraorbital area with 1-2 separated, flat to conical, spines; postorbital with a conical spine near upper anterior angle of opercle; median dorsal head ridges elevated strongly, distal margin of the frontal ridge with a deep notch, the other ridges

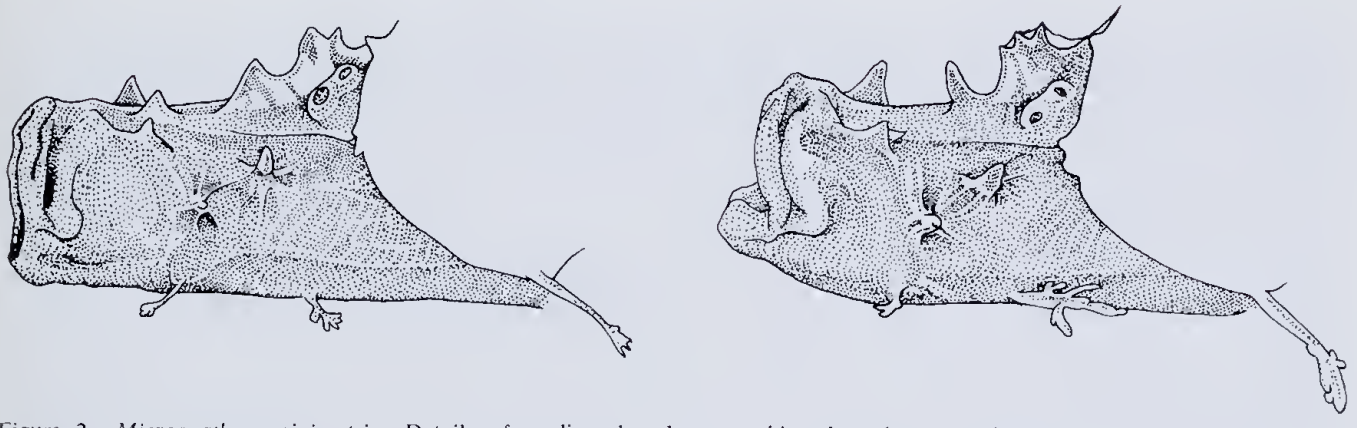

Figure 2.—*Micrognathus spinirostris*. Details of median dorsal snout ridge, lateral snout spines and dermal flaps in holotype (left) and paratype (right).

denticulate. Opercular ridge complete, angled dorsad towards upper posterior angle; opercle elsewhere ornamented with minute striae.

Pectoral-fin base protrudes laterad, the upper ridge reduced to a small conical anterior spine, the lower ridge prominent throughout. Body ridges distinct, notched or indented between rings; superior ridges elevated above dorsum, angled dorsoposteriad on each ring, the edges smooth to denticulate in front but usually with a distinct distal notch and terminal spine; margins of other ridges mostly denticulate but without subterminal notch; scutella without longitudinal keel, prominent in holotype but rather indistinct in paratype. Holotype with pouch plates angled somewhat laterad, brood pouch developed below 13 tail rings, membranes little enlarged and type of pouch closure unknown.

Head with short simple dermal flaps on eye, with elongate branching flaps on side of snout, suborbital, and median dorsal head ridges; with a small branching flap on the inferior ridge of the pectoral-fin base. Holotype with short branching flaps originating on notches in superior ridges of 4th and 8th trunk rings and with similar flaps on posterior part of lateral ridges of 4th trunk ring. Principal axis of branching flaps round or oval in cross section, the distal extremities of branches not expanded or pad-like.

Ground colour of holotype (Fig. 3) now light tan in alcohol; head blotched or irregularly mottled with brown; dorsum and sides of trunk with indications of about 4 broad (3-4 ring) mottled brownish bars and narrow (one ring) pale interspaces; similar bars persists on anterior portion of tail but the distal third is pale throughout; venter of head and several anterior trunk rings mottled with brown, venter elsewhere pale. Dorsal and pectoral rays edged narrowly with brown, the membranes hyaline; caudal fin pale. The elongate dermal flaps sometimes with brown shading near base, otherwise pale. A colour photograph of the fresh specimen shows similar markings and general colouration and and there are 10 narrow pale bars (interspaces) on the side of body behind the pectoral-fin base.

Etymology: Named *spinirostris,* an adjective, in reference to the spiny armature of the snout.

Comparisons: Among nominal Indo-Pacific congeners, *M. spinirostris* shares the modal count of 14 trunk rings, upturned opercular ridge and presence of one or more lateral spines or projections on snout with *M. nitidus* (Günther), *M. brocki* Herald and *M. dunckeri* (Chabanaud). The combination of a discontinuous median dorsal snout ridge, notched superior body ridges and counts of 13-14 pectoral-fin rays separates *M. spinirostris* from *M. dunckeri,* wherein the snout ridge is elevated and continuous, superior ridges are not notched and pectoral-fin rays are modally 11. Both *M. brocki* and *M. nitidus* agree with *M. spinirostris* in that superior ridges are notched on at least some rings. However, the presence of three lateral snout spines, 1-2 spines on the posterior supraorbital and one on the postorbital distinguishes subadult and adult *M. spinirostris* from similar specimens of these species, wherein there are but 1-2 lateral snout spines and spines are absent from the postorbital and posterior supraorbital. Furthermore, *M. brocki* has 21-23 dorsal- and modally 12 pectoral-fin rays (respectively, 19-20 and usually 14 in *spinirostris*) and *M. nitidus* has 29-32 tail rings (33-35 in *spinirostris).* The present species is perhaps most similar to *M. nitidus* in general morphology, but the latter further differs in presence of simple rather than branching dermal flaps and has characteristic alternating narrow bands of pale and dark brown (absent in *spinirostris*).

The Indo-Pacific *M. mataafae* (Jordan and Seale) is also superficially similar to *M. spinirostris.* It differs, however, in having a modal count of 15 trunk rings and only 1-2 lateral snout spines. It lacks the posterior supraopercular spines and superior ridges are not notched.

Remarks: Fritzsche (1975) noted ontogenetic development of spines on the snout of the doryrhamphine (trunk-pouch) pipefish *Doryrhamphus melanopleura* and suggested that similar development occurs in the median dorsal snout ridge of *Micrognathus brachyrhinus* Herald. Among present material, two specimens show differences which suggest that development of the snout ridge, head spines and notches in superior ridges is also ontogenetic in *M. spinirostris.* A 23.8 m SL specimen (USNM 220882) agrees with the type material in having elongate branching flaps on the head, short flaps on the eye and flaps at the posterodorsal angles of some trunk rings. However, the median dorsal snout ridge is represented by two elevated protrusions which are united basally by an emarginate septum and their margins are entire. Furthermore, there appears to be only two developed lateral snout spines, the postorbi-

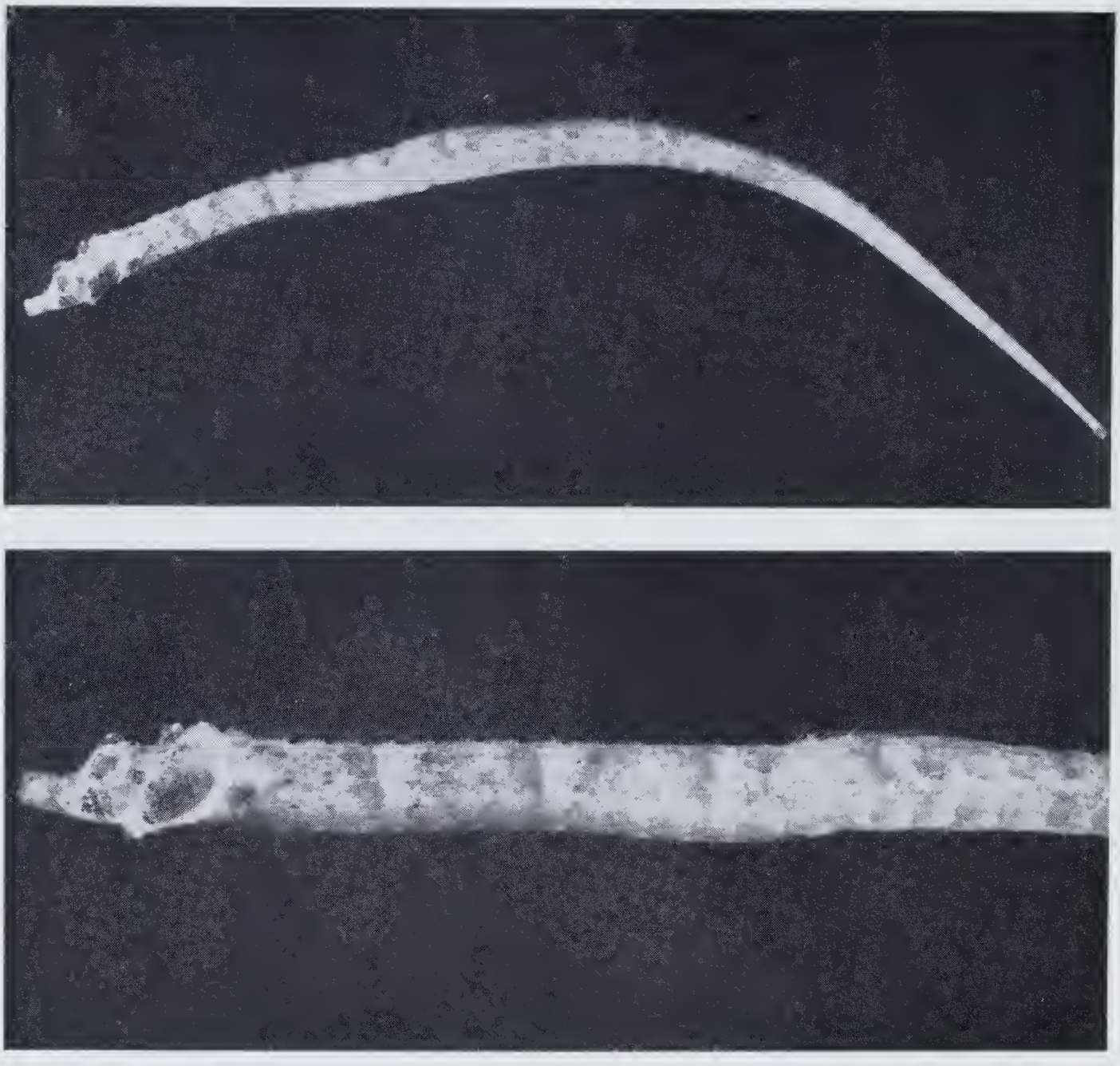

Figure 3.—*Micrognathus spinirostris*. WAM P.26479-001 (103 mm SL, holotype).

tal spine is vestigal and the posterior supraorbital is crossed by a flared ridge. Although superior ridges are angled strongly posterodorsad on each ring, the margins are entire and lack the subterminal notch. A 62.5 mm SL fish (ANSP 142643) has a tripartite median snout ridge but the posterior element is not notched distally and three lateral snout spines are present. Unlike the holotype and paratype, this specimen has but one posterior supraorbital spine and subterminal notches are developed only on the superior trunk ridges. A decaudate male (BPBM 18718) agrees with the holotype in all essential features.

Known specimens of *M. spinirostris* were taken with ichthyocide in SCUBA assisted collections within a range of 4.6-10 m over rock or coral bottom.

Acknowledgments.—For the loan of material in their care, we thank J. E. Bohlke (ANSP), J. E. Randall (BPBM) and E. A. Lachner and associates (USNM). Drawings are by Mrs. Nancy Gordon. This study was in part supported by National Science Foundation Grant BMS 75-19502; C. E. Dawson, principal investigator.

References

Dawson, C. E. (1977).—Synopsis of syngnathine pipefishes usually referred to the genus *Ichthyocampus* Kaup, with description of new genera and species. *Bull. Mar. Sci.*, **27**: 595-650.

Fritzsche, R. A. (1975).—First description of the adult male of *Micrognathus brachyrhinus* (Pisces: Syngnathidae). *Pac. Sci.*, **29**: 267-268.

Herald, E. S. (1953).—Family Syngnathidae: Pipefishes. *in* L. P. Schultz *et al.*, Fishes of the Marshall and Marianas Islands. *Bull. U.S. Nat. Mus.*, **202**: 231-278.

Herald, E. S. and Randall, J. E. (1972).—Five new Indo-Pacific pipefishes. *Proc. Calif. Acad. Sci.*, 4th Ser., **39**: 121-140.

INSTRUCTIONS TO AUTHORS

Contributions to this Journal should be sent to *The Honorary Editor, Royal Society of Western Australia, Western Australian Museum, Francis Street, Perth, Western Australia* 6000. Publication in the Society's Journal is available to all categories of members and to non-members residing outside Western Australia. Where all authors of a paper live in Western Australia at least one author must be a member of the Society. Papers by non-members living outside the State must be communicated through an Ordinary or an Honorary Member. Council decides whether any contribution will be accepted for publication. All papers accepted must be read either in full or in abstract or be tabled at an ordinary meeting before publication.

Papers should be accompanied by a table of contents, on a separate sheet, showing clearly the status of all headings; this will not necessarily be published. Authors should maintain a proper balance between length and substance, and papers longer than 10 000 words would need to be of exceptional importance to be considered for publication. The Abstract (which will probably be read more than any other part of the paper) should not be an expanded title, but should include the main substance of the paper in a condensed form.

Typescripts should be double-spaced on opaque white paper; the original and one copy should be sent. Tables and captions for Figures should be on separate sheets. All pages should be serially numbered. Authors are advised to use recent issues of the Journal as a guide to the general format of their papers, including the preparation of references; journal titles in references may be given in full or may follow any widely used conventional system of abbreviation.

Note that *all* illustrations are Figures, which are numbered in a single sequence. In composite Figures, made up of several photographs or diagrams, each of these should be designated by letter (e.g. Figure 13B). Illustrations should include all necessary lettering, and must be suitable for direct photographic reproduction. No lettering should be smaller than 1 mm on reduction. To avoid unnecessary handling of the original illustrations, which are usually best prepared between $1\frac{1}{2}$ and 2 times the required size, authors are advised to supply extra prints already reduced. Additional printing costs, such as those for folding maps or colour blocks, will normally be charged to authors.

The metric system (S.I. units) must be used in the paper. Taxonomic papers must follow the appropriate International Code of Nomenclature, and geological papers must adhere to the International Stratigraphic Guide. Spelling should follow the Concise Oxford Dictionary.

Extensive sets of data, such as large tables or long appendices, may be classed as Supplementary Publications and not printed with the paper. Supplementary Publications will be lodged with the Society's Library (c/- Western Australian Museum, Perth, W.A. 6000) and with the National Library of Australia (Manuscript Section, Parkes Place, Barton, A.C.T. 2600) and photocopies may be obtained from either institution upon payment of a fee.

Fifty reprints of each paper are supplied free of charge. Further reprints may be ordered at cost, provided that orders are submitted with the returned galley proofs.

Authors are solely responsible for the accuracy of all information in their papers, and for any opinion they express.

Journal

of the

Royal Society of Western Australia

Volume 64 1981

Part 2

Contents

Editor: A. E. Cockbain

No claim for non-receipt of the Journal will be entertained unless it is received within 12 months after publication of part 4 of each volume.

The Royal Society of Western Australia, Western Australian Museum, Perth

11558/3/81—650 WILLIAM C. BROWN, Government Printer